

# CHANNEL-AWARE CONTRASTIVE CONDITIONAL DIFFUSION FOR MULTIVARIATE PROBABILISTIC TIME SERIES FORECASTING

Siyang Li<sup>1</sup>, Yize Chen<sup>2</sup>, Hui Xiong<sup>1\*</sup>

<sup>1</sup>Hong Kong University of Science and Technology (Guangzhou)

<sup>2</sup>University of Alberta

sli572@connect.hkust-gz.edu.cn, yize.chen@ualberta.ca,

xionghui@hkust-gz.edu.cn

## ABSTRACT

Forecasting faithful trajectories of multivariate time series from practical scopes is essential for reasonable decision-making. Recent methods majorly tailor generative conditional diffusion models to estimate the target temporal predictive distribution. However, it remains an obstacle to enhance the exploitation efficiency of given implicit temporal predictive information to bolster conditional diffusion learning. To this end, we propose a generic channel-aware Contrastive Conditional Diffusion model entitled **CCDM** to achieve desirable Multivariate probabilistic forecasting, obviating the need for curated temporal conditioning inductive biases. In detail, we first design a channel-centric conditional denoising network to manage intra-variate variations and cross-variate correlations, which can lead to scalability on diverse prediction horizons and channel numbers. Then, we devise an ad-hoc denoising-based temporal contrastive learning to explicitly amplify the predictive mutual information between past observations and future forecasts. It can coherently complement naive step-wise denoising diffusion training and improve the forecasting accuracy and generality on unknown test time series. Besides, we offer theoretic insights on the benefits of such auxiliary contrastive training refinement from both neural mutual information and temporal distribution generalization aspects. The proposed CCDM can exhibit superior forecasting capability compared to current state-of-the-art diffusion forecasters over a comprehensive benchmark, with best MSE and CRPS outcomes on 66.67% and 83.33% cases. Our code is publicly available at <https://github.com/LSY-Cython/CCDM>.

## 1 INTRODUCTION

Multivariate probabilistic time series forecasting aims to quantify the stochastic temporal evolutions of multiple continuous variables and benefit decision-making in various engineering fields, such as weather prediction (Li et al., 2024), renewable energy dispatch (Dumas et al., 2022), traffic planning (Huang et al., 2023) and financial trading (Gao et al., 2024). Modern methods majorly customize time series generative models (Salinas et al., 2019; Li et al., 2022; Yoon et al., 2019; Rasul et al., 2020) and produce diverse plausible trajectories to decipher the intricate temporal predictive distribution which is conditioned on past observations. Due to the excellent mode coverage capacity and training stability of diffusion models (Song et al., 2020; Ho et al., 2020), a flurry of conditional diffusion forecasters (Lin et al., 2023; Yang et al., 2024) are recently developed by designing effective temporal conditioning mechanisms to discover informative patterns from historical time series.

Despite current advances, there remain two open challenges on learning a precise and generalizable multivariate predictive distribution via the step-wise denoising paradigm. The first obstacle is how to represent *multivariate temporal correlations* in both past observed and target denoised sequences. To this end, many diffusion forecasting methods focus on *efficient architectural designs* upon conditional denoising networks to capture heterogeneous temporal correlations in both diffusion corrupted

---

\*Corresponding author.

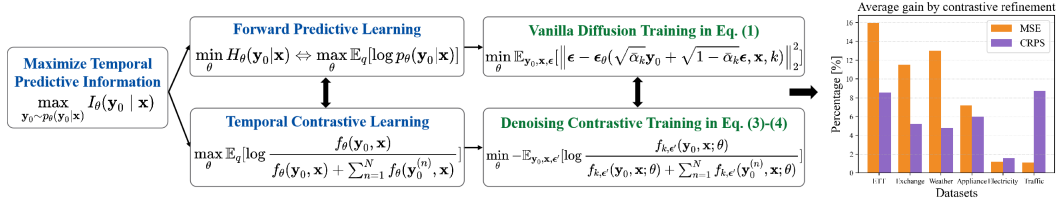


Figure 1: The schematic of proposed information-theoretic denoising-based contrastive diffusion learning. Bi-directional arrows indicate two learning ways are complementary. The bar chart depicts the average gains by contrastive diffusion refinement on diverse prediction setups for six datasets.

and pure conditioning time series. Among them, spatiotemporal attention layers in CSDI (Tashiro et al., 2021) and structured state space modules in SSSD (Alcaraz & Strodthoff, 2022) are employed to characterize intra-channel and inter-channel<sup>1</sup> relations. LDT (Feng et al., 2024) and D<sup>3</sup>VAE (Li et al., 2022) utilize latent diffusion models to handle high-dimensional sequences. However, due to the limited capacity on identifying channel-specific and cross-channel properties, these temporal denoisers cannot manifest scalability and reliability on tough prediction tasks with numerous channels or long terms. Inspired by recent success of channel-centric views in multivariate point forecasting (Chen et al., 2024a; Liu et al., 2023), we propose to endow a *unified channel manipulation strategy* into the conditional denoising network, as depicted in Fig. 3, where we stack channel-independent and channel-mixing modules to capture univariate variations and inter-variate correlations.

The second issue is how to enhance the *exploitation efficiency of the implicit predictive information* hidden in provided time series, which can improve the diversity and accuracy of generated profiles. It has been revealed that learning to unveil the useful temporal information like decomposed patterns (Deng et al., 2024) or spectral biases (Crabbé et al., 2024) can boost the estimated predictive distribution. Related diffusion forecasters also develop *auxiliary training strategies* to amplify the fine-grained features, as the naive step-wise noise regression paradigm fall short in fully releasing the intrinsic predictive information. In particular, they employ specific temporal inductive biases to promote temporal conditioning schemes or guide iterative inference procedures. Pretraining temporal conditioning encoders by deterministic point prediction (Shen & Kwok, 2023; Li et al., 2023) is a viable method, which produces more accurate medians and sharper prediction intervals. Coupling unique temporal features like multi-granularity dynamics (Fan et al., 2024; Shen et al., 2023) or target quantitative metrics (Kollovich et al., 2024) to regularize the sequential diffusion process can also steer the reverse generation process towards plausible trajectories. However, these auxiliary methods need to fully expose task-specific temporal properties or tailor distinct regulations for diffusion training and sampling procedures. They are neither consistent with standard hierarchical diffusion optimization nor generic over generative time series diffusion models.

Motivated by a neural information view in (Tsai et al., 2020), naive conditional time series diffusion learning can be deemed as a *forward predictive way* to maximize the temporal mutual information between past observations and target forecasts. Such auxiliary inductive biases can empirically enrich the predictive temporal information. However, single predictive learning is inadequate to reveal the entire task-specific information. In light of the composite objective which integrates contrastive learning to procure more robust task-related representations (Tsai et al., 2020), we propose to further enhance the *prediction-related mutual information* captured by denoising diffusion in a *complementary contrastive way*, where both positive and negative time series are inspected at each diffusion step. We illustrate such temporal contrastive refinement on conditional diffusion forecasting in Fig. 1, which mitigates over-fitting and attains better generality on unknown test data.

In this work, we propose a contrastive conditional diffusion model termed CCDM which can explicitly maximize the predictive mutual information for multivariate probabilistic forecasting. The efficient *channel-aware denoiser architecture* and complementary *denoising-based contrastive refinement* are two recipes to boost diffusion forecasting capacity. Our main contributions are summarized as: (1) We design a composite channel-aware conditional denoising network, which merges channel-independent dense encoders to extract univariate dynamics and channel-wise diffusion transformers to aggregate cross-variate correlations. It gives rise to efficient iterative inference and better scalability on various channel numbers and prediction horizons. (2) We propose to explicitly amplify the predictive information between generated forecasts and past observations via a coherent denoising-

<sup>1</sup>A channel shares the same physical interpretations with a variate, with each channel indicating a univariate time series.

based temporal contrastive learning, which can be seamlessly aligned with vanilla step-wise denoising diffusion training and thus efficient to implement. (3) Extensive simulations validate the superior forecasting capability of CCDM. It can attain better accuracy and reliability versus other excellent models on various forecasting settings, especially for long-term and large-channel scenarios.

## 2 PRELIMINARIES

### 2.1 PROBLEM FORMULATION

In this paper, we look into the task of multivariate probabilistic time series forecasting. Given the past observation  $\mathbf{x} \in \mathbb{R}^{L \times D}$  as conditioning time series, the goal is to generate a group of  $S$  plausible forecasts  $\{\hat{\mathbf{y}}_0^{(s)} \in \mathbb{R}^{H \times D}\}_{s=1}^S$  from the learned conditional predictive distribution  $p_\theta(\mathbf{y}_0|\mathbf{x})$ . Here,  $D$  is the number of channels,  $L$  and  $H$  indicate the lookback window length and prediction horizon respectively.  $\theta$  stands for the parameters of a conditional diffusion forecaster which represents the real predictive distribution  $q(\mathbf{y}_0|\mathbf{x})$ . We allocate diverse values to horizon  $H$  and channel number  $D$  to construct a holistic benchmark which can completely evaluate the capability of different conditional diffusion models on various forecasting scenarios.

### 2.2 CONDITIONAL DENOISING DIFFUSION MODELS

Conditional diffusion models have exhibited impressive capability on a wide variety of controllable multi-modal synthesis tasks (Chen et al., 2024b). It dictates a bi-directional distribution transport process between raw data  $\mathbf{y}_0$  and prior Gaussian noise  $\mathbf{y}_K \in \mathcal{N}(\mathbf{0}, \mathbf{I})$  via  $K$  diffusion steps. The forward process gradually degrades clean  $\mathbf{y}_0$  to fully noisy  $\mathbf{y}_K$  and can be fixed as a Markov chain:  $q(\mathbf{y}_{0:K}) = q(\mathbf{y}_0) \prod_{k=1}^K q(\mathbf{y}_k|\mathbf{y}_{k-1})$ , where  $q(\mathbf{y}_k|\mathbf{y}_{k-1}) := \mathcal{N}(\mathbf{y}_k; \sqrt{1 - \beta_k}\mathbf{y}_{k-1}, \beta_k\mathbf{I})$  and  $\beta_k$  is the degree of imposed step-wise Gaussian noise. We can accelerate the forward sampling procedure and obtain closed-form latent state  $\mathbf{y}_k$  at arbitrary step  $k$  by a noteworthy property (Ho et al., 2020):  $\mathbf{y}_k = \sqrt{\bar{\alpha}_k}\mathbf{y}_0 + \sqrt{1 - \bar{\alpha}_k}\boldsymbol{\epsilon}$ , where  $\bar{\alpha}_k := \prod_{s=1}^k (1 - \beta_s)$  and  $\boldsymbol{\epsilon} \sim \mathcal{N}(\mathbf{0}, \mathbf{I})$ . The reverse generation process converts known Gaussian to realistic prediction data  $\mathbf{y}_0$  given input conditions  $\mathbf{x}$ , which can be cast as a parameterized Markov chain:  $p_\theta(\mathbf{y}_{0:K}|\mathbf{x}) = p(\mathbf{y}_K) \prod_{k=K}^1 p_\theta(\mathbf{y}_{k-1}|\mathbf{y}_k, \mathbf{x})$ . The overall training objective can be simplified as minimizing the step-wise denoising loss below:

$$\mathcal{L}_k^{denoise} = \mathbb{E}_{\mathbf{y}_0, \mathbf{x}, \boldsymbol{\epsilon}} [\|\boldsymbol{\epsilon} - \boldsymbol{\epsilon}_\theta(\sqrt{\bar{\alpha}_k}\mathbf{y}_0 + \sqrt{1 - \bar{\alpha}_k}\boldsymbol{\epsilon}, \mathbf{x}, k)\|_2^2]. \quad (1)$$

A potential issue for current conditional diffusion models lies in forging an effective conditioning mechanism that can enhance the alignment between given conditions  $\mathbf{x}$  and produced data  $\mathbf{y}_0$ , like the coherent semantics between textual descriptions and visual renderings (Esser et al., 2024), or the conformity of generated vehicle motions to scenario constraints (Jiang et al., 2023). However, such data consistency is hard to represent for temporal conditional probability modeling. We thus explicitly learn to amplify the prediction-related temporal information conveyed from past conditioning time series to generated trajectories. Such predictive mutual information can reflect underlying temporal properties in historical sequences, to which the produced forecasts should comply.

### 2.3 NEURAL MUTUAL INFORMATION MAXIMIZATION

As discussed above, to more efficiently represent the useful predictive modes involved in conditioning time series, we choose to explicitly maximize the prediction-oriented mutual information when learning the conditional diffusion forecaster. Learning to maximize mutual information is effective to boost the consistency between two associated variables (Song & Ermon, 2019), which has been actively applied to self-supervised learning (Liang et al., 2024b) and multi-modal alignment (Liang et al., 2024a). Regarding conditional diffusion learning, there also exist several related works (Wang et al., 2023; Zhu et al., 2022) which explicitly employ mutual information maximization to enhance high-level semantic coherence between input prompts and generated samples. While we propose a complementary way to equip the conditional diffusion forecaster with this tool to bolster the utilization of informative temporal patterns. Besides, we provide a distinct composite loss design and more concrete interpretations on the benefits of the contrastive scheme to ordinary conditional diffusion.

Among the two practical methods to maximize the intractable mutual information (Tsai et al., 2020), contrastive learning aids to strengthen the association by discriminating intra-class from inter-class

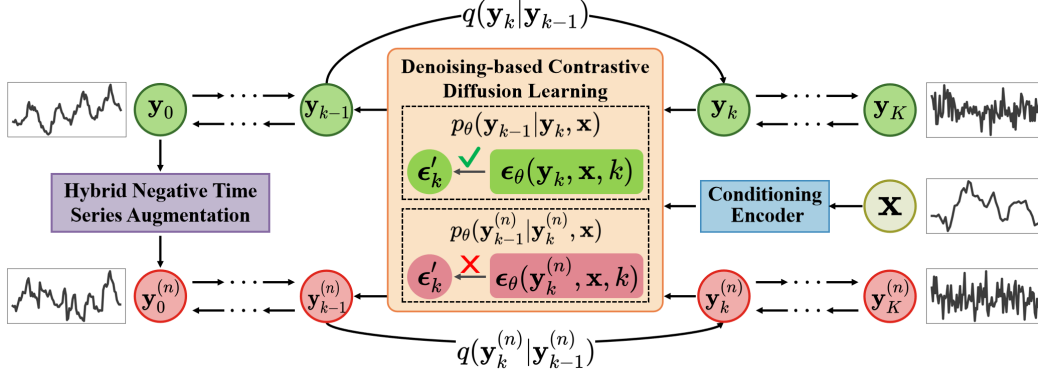


Figure 2: The framework of denoising-based contrastive conditional diffusion forecaster.

samples. Contrastive predictive coding (Oord et al., 2018) realizes such objective by optimizing the contrastive lower bound with low variance via the prevalent InfoNCE loss:

$$\mathcal{L}_{InfoNCE} = -\mathbb{E}_{(y_0, \mathbf{x}) \sim q(y_0, \mathbf{x}), y_0^{(n)} \sim q^n(y_0)} \left[ \log \frac{f(y_0, \mathbf{x})}{f(y_0, \mathbf{x}) + \sum_{n=1}^N f(y_0^{(n)}, \mathbf{x})} \right]. \quad (2)$$

During each iteration, we create a set of  $N$  negative samples via the negative construction operation  $q^n(y_0)$  on positive data  $y_0$ .  $f(y_0, \mathbf{x})$  accounts for the density ratio  $\frac{q(y_0|\mathbf{x})}{q(y_0)}$  and can be *any types of positive real functions*. This flexible form of the density ratio function offers a natural initiative of the following denoising-based contrastive conditional diffusion.

*Forward predictive learning* is another way to boost the inter-dependency by fully reconstructing target  $y_0$  conditioned on given  $\mathbf{x}$ . This reconstruction learning can be realized by learning a deterministic mapping or conditional generative model from  $\mathbf{x}$  to  $y_0$ . As  $I(y_0; \mathbf{x}) = H(y_0) - H(y_0|\mathbf{x})$ , and  $H(y_0)$  is irrelevant to discovering the entanglement between  $\mathbf{x}$  and  $y_0$ , thereby maximizing  $I(\mathbf{x}; y_0)$  boils down to optimizing the predictive lower bound  $-H(y_0|\mathbf{x}) = \mathbb{E}_{q(\mathbf{x}, y_0)} [\log p_\theta(y_0|\mathbf{x})]$ , which is aligned with the likelihood-based objective of naive conditional diffusion learning. (Tsai et al., 2020) claims that combining both predictive and contrastive learning tactics can significantly raise the quality of obtained task-related features. Accordingly, we equip vanilla conditional time series diffusion with a denoising-based InfoNCE contrastive loss to further boost the temporal predictive information between past conditions and future forecasts. A concise motivation of this information-theoretic contrastive diffusion forecasting is depicted in Fig. 1.

### 3 METHOD: CHANNEL-AWARE CONTRASTIVE CONDITIONAL DIFFUSION

In this section, we elucidate two innovations of the tailored CCDM for generative multivariate time series forecasting, including the hybrid channel-aware denoiser architecture depicted in Fig. 3 and denoising-based contrastive diffusion learning demonstrated in Fig. 2.

#### 3.1 CHANNEL-AWARE CONDITIONAL DENOISING NETWORK

Recent progress on multivariate prediction methods (Liu et al., 2023; Ilbert et al., 2024) show that proper integration of channel management strategies in time series backbones is critical to discover univariate dynamics and cross-variate correlations. But this problem has not been well explored in multivariate diffusion forecasting and previous conditional denoiser structures do not obviously distinguish such heterogeneous channel-centric temporal properties. To this end, we design a channel-aware conditional denoising network which incorporates composite channel manipulation modules, i.e. channel-independent dense encoders and channel-mixing diffusion transformers. This architecture can efficiently represent intra-variate and inter-variate temporal correlations in past conditioning  $\mathbf{x}$  and future predicted  $y_0$  under different noise levels, as well as being robust to diverse prediction horizons and channel numbers.

**Channel-independent dense encoders.** We develop two channel-independent MLP encoders to extract unique temporal variations in each individual channel of observed condition  $\mathbf{x}$  and corrupted latent state  $y_k$  at each diffusion step. The core ingredient in latent and condition encoders is the

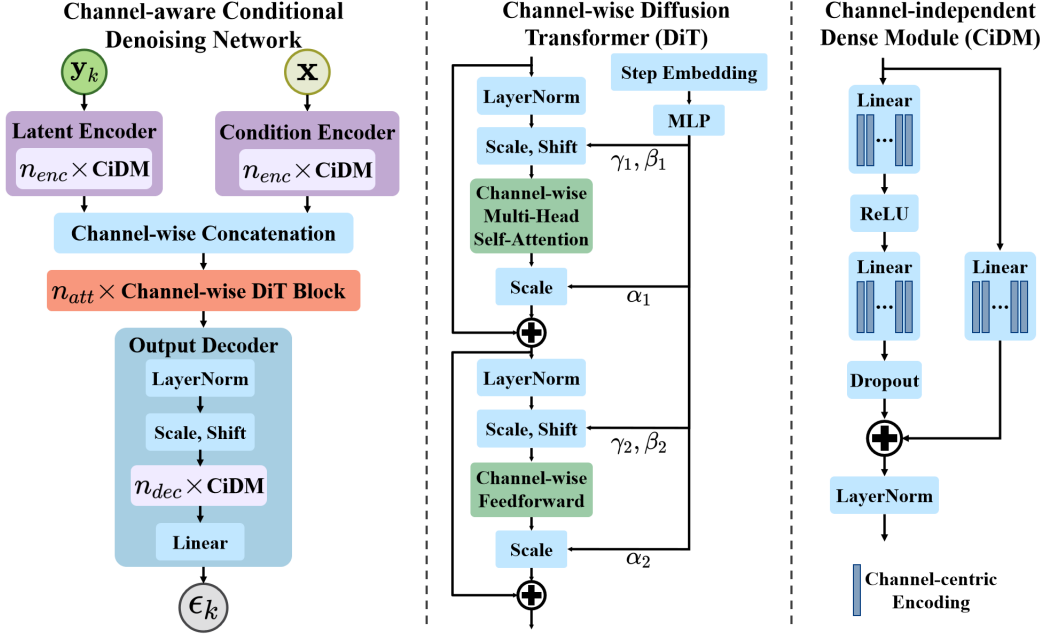


Figure 3: The diagram of channel-aware conditional denoiser architecture. Left: the whole network. Middle: channel-mixing DiT blocks. Right: channel-independent MLP dense modules.

channel-independent dense module (CiDM) borrowed from TiDE (Das et al., 2023a), which stands out as a potent MLP building-block for universal time series analysis models (Das et al., 2023b). A salient element in CiDM is the skip-connecting MLP residual block which can improve temporal pattern expressivity. The  $D$  linear layers in parallel are shared and used for separate channel feature embedding. We stack  $n_{enc}$  CiDM modules of  $e_{hid}$  hidden dimension to transform both  $\mathbf{x}$  and  $\mathbf{y}_k$  into  $e_{hid} \times D$  size. These two input encoders can be easily adjusted to accommodate different context windows and hidden feature dimensions.

**Channel-wise diffusion transformers.** To regress step-wise Gaussian noise  $\epsilon_k$  on raw  $\mathbf{y}_0$  more precisely, we should fully exploit implicit temporal information in pure conditioning  $\mathbf{x}$  and polluted target  $\mathbf{y}_k$ . We concatenate the latent encoding of  $\mathbf{x}$  and  $\mathbf{y}_k$  along the channel axis and then leverage  $n_{att}$ -depth channel-wise diffusion transformer (DiT) blocks to aggregate heterogeneous temporal modes from various channels. DiT is an emergent diffusion backbone for open-ended text-to-image synthesis which merits eminent efficiency, scalability and robustness (Peebles & Xie, 2023; Esser et al., 2024). Two critical components in DiT are multi-head self-attention for feature fusion and adaptive layer norm (adaLN) layers to absorb other conditioning items (e.g. diffusion step embedding, text labels) as learnable scale and shift parameters. Although DiT has been adopted by few works (Cao et al., 2024; Feng et al., 2024) for generative time series modeling, they do not adapt it in a fully channel-centric angle. We repurpose DiT to model multivariate predictive distribution by replacing naive point-wise attention to a channel-wise version, which can blend correlated temporal information from different variates in  $\mathbf{x}$  and  $\mathbf{y}_k$ . Afterwards, we develop an output decoder with  $n_{dec}$  CiDMs plus a last adaLN to yield the prediction of imposed noise  $\epsilon_k$  given  $\mathbf{x}$  and  $\mathbf{y}_k$ .

### 3.2 DENOISING-BASED TEMPORAL CONTRASTIVE REFINEMENT

Unlike previous empirically designed temporal conditioning schemes to make better exploitation of past predictive information, we instead propose to explicitly maximize the prediction-related mutual information  $I(\mathbf{y}_0; \mathbf{x})$  between past observations  $\mathbf{x}$  and future forecasts  $\mathbf{y}_0$  via an adapted denoising-based contrastive strategy. We will employ the learnable denoising network  $\epsilon_\theta(\cdot)$  to represent the contrastive lower bound of  $I(\mathbf{y}_0; \mathbf{x})$  presented by Eq. 2, and exhibit this information-theoretic contrastive refinement is complementary and aligned with original conditional denoising diffusion optimization, which is actually another forward predictive method to maximize  $I(\mathbf{y}_0; \mathbf{x})$ .

To improve the diffusion forecasting capacity more essentially, the developed contrastive learning item is wished to directly benefit naive step-wise denoising-based training procedure, i.e. regular-

izing noise elimination behaviors of the conditional denoiser  $\epsilon_\theta(\cdot)$ . Since the density ratio function  $f(\mathbf{y}_0, \mathbf{x})$  constituting the contrastive mutual information lower bound in Eq. 2 can be any positive-valued forms, this flexibility naturally motivates us to prescribe  $f(\cdot)$  using the step-wise denoising objective in Eq. 1, for both positive sample  $\mathbf{y}_0$  and a group of negative samples  $\mathbf{y}_0^{(n)}$ :

$$f_{k,\epsilon'}(\mathbf{y}_0, \mathbf{x}; \theta) = \exp(-\|\epsilon' - \epsilon_\theta(\sqrt{\alpha_k}\mathbf{y}_0 + \sqrt{1-\alpha_k}\epsilon', \mathbf{x}, k)\|_2^2/\tau); \quad (3a)$$

$$f_{k,\epsilon'}(\mathbf{y}_0^{(n)}, \mathbf{x}; \theta) = \exp(-\|\epsilon' - \epsilon_\theta(\sqrt{\alpha_k}\mathbf{y}_0^{(n)} + \sqrt{1-\alpha_k}\epsilon', \mathbf{x}, k)\|_2^2/\tau); \quad (3b)$$

where  $\tau$  is the temperature coefficient in the softmax-form contrastive loss. The negative sample set  $\{\mathbf{y}_0^{(n)}\}_{n=1}^N$  is constructed by a hybrid time series augmentation method which alters both temporal variations and point magnitudes (See Appendix A.3 for details.). Then, we can derive the following contrastive refinement loss which is coincident with vanilla step-wise denoising diffusion training:

$$\mathcal{L}_k^{contrast} = -\mathbb{E}_{\mathbf{x}, \mathbf{y}_0, \{\mathbf{y}_0^{(n)}\}_{n=1}^N, \epsilon'} [\log \frac{f_{k,\epsilon'}(\mathbf{y}_0, \mathbf{x}; \theta)}{f_{k,\epsilon'}(\mathbf{y}_0, \mathbf{x}; \theta) + \sum_{n=1}^N f_{k,\epsilon'}(\mathbf{y}_0^{(n)}, \mathbf{x}; \theta)}]. \quad (4)$$

Apparently, the devised denoising-based temporal contrastive learning can not only seamlessly coordinate with standard diffusion training at each step  $k$ , but also improve the conditional denoiser behaviors in out-of-distribution (OOD) regions. These OOD areas are constituted by the low-density diffusion paths of negative samples, which are not touched by merely executing denoising learning along the high-density probability paths of positive samples.

### 3.3 OVERALL LEARNING OBJECTIVE

The naive denoising diffusion model trained by log-likelihood maximization (Ho et al., 2020) totally owns  $K$ -step valid training items. To align with this step-wise denoising distribution learning, we can amortize the contrastive regularization in Eq. 4 to each training step, and derive the overall learning objective below:

$$\max_{\theta} \mathbb{E}_{q(\mathbf{y}_0, \mathbf{x})} [\log p_\theta(\mathbf{y}_0|\mathbf{x}) + \lambda K \cdot I_\theta(\mathbf{y}_0; \mathbf{x})], \quad (5)$$

where  $\log p_\theta(\mathbf{y}_0|\mathbf{x})$  can be decomposed as  $\sum_{k=1}^K \mathcal{L}_k^{denoise}$  and indicates the predictive distribution learning. Whilst  $\max_{\theta} I_\theta(\mathbf{y}_0; \mathbf{x})$  governs the information-theoretic contrastive learning. Then, the practical training loss of the devised CCDM at each diffusion step can be presented as:

$$\mathcal{L}_k^{CCDM} = \mathbb{E}_{\mathbf{y}_0, \mathbf{x}, k \sim U[1, K]} (\mathcal{L}_k^{denoise} + \lambda \mathcal{L}_k^{contrast}). \quad (6)$$

So far, we obtain the overall step-wise training procedure for CCDM, which is a  $\lambda$ -weighted combination of the vanilla denoising term in Eq. 1 and auxiliary contrastive item in Eq. 4. The whole training algorithm is clarified in Appendix A.4, which is efficient, end-to-end and seamlessly coupled with original simplified denoising diffusion.

**Theoretical insights.** Beyond the concrete method described above, we offer two-fold interpretations on how conditional diffusion forecasters can gain from auxiliary temporal contrastive learning. From the *neural mutual information perspective*, Eq. 1 and Eq. 4 train the parameterized conditional denoiser  $\epsilon_\theta(\cdot)$  to simultaneously optimize two complementary lower bounds (i.e. predictive and contrastive) of the prediction-related mutual information  $I_\theta(\mathbf{y}_0; \mathbf{x})$  between future forecasts and past conditioning time series. According to (Tsai et al., 2020), this composite learning method can enhance the representation efficiency to distill task-related information from accessible conditions. The contrastive scheme assists  $\epsilon_\theta(\cdot)$  to learn helpful negative instances, which can gain useful discriminative temporal patterns for accurate multivariate predictive distribution recovery and mitigate over-fitting on historical training time series. From the *distribution generalization perspective*, explicitly optimizing the probabilities of unexpected negative samples can render  $\epsilon_\theta(\cdot)$  see more OOD regions that pure denoising fashion on positive in-distribution samples do not encompass. In time series forecasting, there always exists distribution shift between unforeseen testing data and historical training data. The contrastive term in Eq. 4 intuitively minimizes the possibility  $\log p_\theta(\mathbf{y}_0^{(n)})$  of undesirable spurious forecasts by directly impeding  $\epsilon_\theta(\cdot)$  from correctly removing the noise over negative  $\mathbf{y}_0^{(n)}$ . This contrastive enforcement helps  $\epsilon_\theta(\cdot)$  avoid low-density areas and undergo more OOD areas during in-distribution training. In light of the arguments in (Wu et al., 2024), promoting the denoiser robustness in OOD regions in testing stage is crucial to sample plausible forecasts.

Moreover, we reveal the upper bound of forecasting error on testing data for conditional diffusion models in Proposition 1. It obviously reflects that the efficacy of conditional diffusion forecasters is inextricably intertwined with the step-wise noise regression accuracy of trained  $\epsilon_\theta(\cdot)$  on unknown test time series. In this regard, resorting to temporal contrastive refinement or other auxiliary training regimes is sensible to boost conditional denoiser behaviors and final prediction outcomes.

**Proposition 1.** *Let  $q^{te}(\mathbf{y}_0|\mathbf{x})$  be the ground truth distribution of test time series, and  $p_\theta^{te}(\mathbf{y}_0|\mathbf{x})$  be the approximated predictive distribution by the developed conditional diffusion model. Let the KL-divergence between  $q^{te}(\mathbf{y}_0|\mathbf{x})$  and  $p_\theta^{te}(\mathbf{y}_0|\mathbf{x})$  represent the resulting probabilistic forecasting error. Then the denoising diffusion-induced forecasting error is upper-bounded:*

$$\mathcal{D}_{KL} [q^{te}(\mathbf{y}_0|\mathbf{x})||p_\theta^{te}(\mathbf{y}_0|\mathbf{x})] \leq \mathbb{E}_{\mathbf{x}, \mathbf{y}_0, \epsilon_k, k} \left[ A_k \left\| \epsilon_\theta \left( \sqrt{\bar{\alpha}_k} \mathbf{y}_0 + \sqrt{1 - \bar{\alpha}_k} \epsilon_k, \mathbf{x}, k \right) - \epsilon_k \right\|_2^2 \right] + C. \quad (7)$$

*Such upper bound is determined by the denoising behaviors of learned  $\epsilon_\theta(\cdot)$  on unknown test time series.  $A_k$  is a step-wise constant related to noise schedule, and  $C$  is a constant depending on test data quantities. See Appendix A.1 for the proof.*

## 4 EXPERIMENTS

### 4.1 EXPERIMENTAL SETUP

**Datasets.** We choose six multivariate time series datasets, i.e. ETTh1, Exchange, Weather, Appliance, Electricity, Traffic, which cover a wide range of temporal dynamics and channel number  $D$  to completely gauge the probabilistic forecasting performance. We manually establish a more comprehensive benchmark with diverse values of lookback window  $L$  and prediction horizon  $H$ , distinct from previous models which merely attest their generative forecasting capacity on a single short-term setup. Refer to Appendix. A.5 for more details on datasets.

**Evaluation metrics.** We adopt two standard metrics to assess the quality of both probabilistic and deterministic forecasts resulting from the generated prediction intervals. CRPS (Continuous Ranked Probability Score) is used to assess the reliability of the estimated predictive distribution, and MSE (Mean Squared Error) is used to quantify the accuracy of calculated point forecasts. See Appendix A.6 for more details on metrics.

**Baselines.** We select five currently remarkable denoising diffusion-based generative forecasters for comparisons, including TimeGrad (Rasul et al., 2021), CSDI (Tashiro et al., 2021), SSSD (Alcaraz & Strodthoff, 2022), TimeDiff (Shen & Kwok, 2023), TMDM (Li et al., 2023). Since these models do not shed light on outcomes on long-term probabilistic forecasting scenarios, we fully reproduce them on the newly constructed benchmark.

**Implementation details.** We normally execute the end-to-end contrastive diffusion training in Eq. 6 using 200 epochs. To reduce the contrastive learning costs on those cases which consume enormous computational resources, we also employ a cost-efficient two-stage training strategy. Concretely, we firstly pretrain a low-cost naive diffusion forecaster by Eq. 1 and fine-tune it by the total contrastive manner in Eq. 6 with only 30 epochs. We keep the temperature coefficient  $\tau = 0.1$  and randomly generate  $S = 100$  multivariate profiles to compose prediction intervals. See Appendix A.7 for more details on network architecture and contrastive training configurations in different forecasting setups. All experiments are conducted on a single NVIDIA A100 40GB GPU.

### 4.2 OVERALL RESULTS

We demonstrate the devised CCDM model can outperform existing diffusion forecasters on most of the generative forecasting cases in Table 1. Concretely, CCDM can attain the best outcomes on 16/24 deterministic and 20/24 probabilistic evaluations, with 9.10% and 15.66% average improvement of MSE and CRPS on these cases. Especially on two most difficult datasets *Electricity* and *Traffic*, CCDM garners notable progress of 8.94%, 10.59% on MSE and 19.73%, 19.10% on CRPS. These prominent increases reflect the devised channel-centric structure and contrastive refinement on the diffusion forecaster can enhance its representation efficiency of implicit predictive information on diverse prediction scenarios. The second-best model CSDI also manifests excellent forecasting ability especially on *Weather*, which has complex multivariate temporal correlations.

Table 1: Overall comparisons w.r.t MSE and CRPS on six real-world datasets with diverse horizon  $H \in \{96, 168, 336, 720\}$ . The best and second-best results are boldfaced and underlined.

Methods		CCDM		TMDM		TimeDiff		SSSD		CSDI		TimeGrad	
Metrics		MSE	CRPS	MSE	CRPS	MSE	CRPS	MSE	CRPS	MSE	CRPS	MSE	CRPS
ETTh1	96	<b>0.3856</b>	<b>0.2935</b>	0.4692	0.3952	0.4025	0.3942	1.0984	0.5622	1.1013	0.5794	1.1730	0.6223
	168	<b>0.4267</b>	<b>0.3142</b>	0.5296	0.4163	<u>0.4397</u>	<u>0.4170</u>	0.6067	<u>0.4046</u>	1.1013	0.5794	1.1554	0.5970
	336	<u>0.5312</u>	<b>0.3452</b>	0.5862	0.4655	<b>0.4943</b>	<u>0.4488</u>	0.9330	<u>0.5421</u>	1.0459	0.6223	1.1403	0.5883
	720	<b>0.5642</b>	<b>0.4870</b>	0.7083	0.5335	<u>0.5779</u>	<u>0.5145</u>	1.3776	0.7035	1.0081	0.5952	1.2529	0.6498
	Avg	<b>0.4769</b>	<b>0.3600</b>	0.5733	0.4526	<u>0.4786</u>	<u>0.4418</u>	1.0039	0.5531	1.0642	0.5941	1.1804	0.6144
Exchange	96	<b>0.0905</b>	<b>0.1545</b>	0.1278	0.2112	<u>0.1106</u>	0.2349	0.5551	0.4569	0.2551	0.2901	1.8655	1.0439
	168	<b>0.1638</b>	<b>0.2159</b>	0.2791	0.3210	<u>0.2050</u>	<u>0.3187</u>	0.4517	0.3602	0.8050	0.5093	1.1638	0.8374
	336	<b>0.4407</b>	<b>0.3517</b>	<u>0.4572</u>	0.4426	<u>0.5834</u>	<u>0.5472</u>	0.5641	<u>0.4106</u>	0.6179	0.4786	1.9264	1.0465
	720	1.1685	<b>0.5864</b>	2.5625	1.0828	<b>0.9096</b>	0.7128	1.3686	<u>0.6386</u>	1.3816	0.7423	2.4034	1.1478
	Avg	<u>0.4659</u>	<b>0.3271</b>	0.8567	0.5144	<b>0.4522</b>	<u>0.4534</u>	0.7349	0.4666	0.7649	0.5051	1.8398	1.0189
Weather	96	<u>0.2669</u>	<b>0.1904</b>	0.2768	0.2273	0.3842	0.3441	0.6103	0.3878	<b>0.2608</b>	0.2127	0.5628	0.3445
	168	<b>0.2489</b>	<b>0.2006</b>	0.2864	0.2519	0.3566	0.3192	<u>0.2796</u>	<u>0.2060</u>	0.2930	<u>0.2286</u>	0.4141	0.2880
	336	<b>0.2870</b>	0.2258	0.3494	0.3007	0.4805	0.3591	0.3189	<u>0.2355</u>	<u>0.2918</u>	<b>0.2193</b>	0.5462	0.3549
	720	0.5627	<u>0.4083</u>	<u>0.3975</u>	0.3365	0.5052	0.3880	0.6880	0.4179	<b>0.3803</b>	<b>0.2770</b>	0.4774	<u>0.3221</u>
	Avg	0.3414	<u>0.2563</u>	<u>0.3275</u>	0.2791	0.4316	0.3526	0.4742	0.3118	<b>0.3065</b>	<b>0.2344</b>	0.5001	0.3274
Appliance	96	0.6988	<b>0.4138</b>	0.6858	0.4678	0.7328	0.5740	1.1954	0.6504	<b>0.6823</b>	0.4334	1.6748	0.8397
	168	<b>0.6266</b>	<b>0.4020</b>	0.7153	0.5232	<u>0.6468</u>	0.5562	0.7841	0.4776	0.7176	<u>0.4560</u>	1.8901	0.8858
	336	<b>0.9119</b>	<b>0.5036</b>	1.0310	0.6590	<u>0.9531</u>	0.6822	1.8822	0.8002	1.0565	<u>0.5675</u>	1.8506	0.8661
	720	1.5798	0.8620	<b>1.3937</b>	<u>0.8272</u>	<u>1.4327</u>	0.8809	3.3226	1.1225	1.7347	<b>0.7982</b>	2.4393	1.0083
	Avg	<u>0.9543</u>	<b>0.5454</b>	0.9565	0.6193	<b>0.9414</b>	0.6733	1.7961	0.7627	1.0478	<u>0.5638</u>	1.9637	0.9000
Electricity	96	0.2102	<b>0.2182</b>	<b>0.1954</b>	0.3113	0.1960	0.3123	0.2444	<u>0.2346</u>	0.2560	0.2571	0.3733	0.3259
	168	<b>0.1678</b>	0.2014	0.1908	0.3037	<u>0.1907</u>	0.3043	0.2001	<u>0.2249</u>	<u>0.1754</u>	<b>0.1985</b>	0.3676	0.3083
	336	<b>0.1683</b>	<b>0.2014</b>	0.2042	0.3165	0.2047	0.3172	0.1941	0.2245	<u>0.1803</u>	<u>0.2043</u>	0.4249	0.3497
	720	<b>0.1994</b>	<b>0.2232</b>	0.2282	0.3338	<u>0.2277</u>	<u>0.3336</u>	0.3743	0.3680	0.9932	0.5678	0.4299	0.3479
	Avg	<b>0.1864</b>	<b>0.2111</b>	<u>0.2047</u>	0.3163	0.2048	0.3169	0.2532	<u>0.2630</u>	0.4012	0.3069	0.3989	0.3330
Traffic	96	1.0282	<b>0.4093</b>	<u>0.9692</u>	0.5894	<b>0.9684</b>	0.5859	1.0363	0.4445	1.1154	0.4240	1.2259	0.4667
	168	<b>0.6881</b>	<b>0.3077</b>	0.8632	0.5254	<u>0.8553</u>	0.5192	0.9551	<u>0.4289</u>	1.6000	0.6701	1.3282	0.5510
	336	<b>0.6863</b>	<b>0.3358</b>	0.8874	0.5562	<u>0.8834</u>	0.5538	0.9283	0.5140	1.5724	0.6780	1.0447	0.3817
	720	<b>0.9357</b>	<b>0.4519</b>	<u>1.0258</u>	0.6383	<u>1.0270</u>	0.6387	1.0635	0.5515	1.5428	0.6696	1.1753	<u>0.4604</u>
	Avg	<b>0.8346</b>	<b>0.3762</b>	0.9364	0.5773	<u>0.9335</u>	0.5744	0.9958	0.4847	1.4577	0.6104	1.1935	0.4650

The hybrid attention module in CSDI can well capture these relations but it entices high computational overhead and over-fitting to other datasets. TMDM and TimeDiff also attain small MSE on few cases due to their extra deterministic pre-training operations on conditioning encoders. Note that we completely replicate TimeGrad on the whole benchmark for the first time even with severe inference costs, and validate it can actually realize reasonable forecasting results. In Fig. 4, we depict different diffusion produced prediction intervals on one case. We can clearly see that CCDM’s interval is much more faithful, while TimeDiff’s area is sharper but loses diversity and accuracy. See Appendix A.11 for more forecasting result showcases and Appendix A.8 on time cost analysis.

### 4.3 ABLATION STUDY

To investigate respective effects of each component, we remove the proposed denoising-based contrastive learning and channel-wise DiT structure, and exhibit the average metric degradation over different prediction horizons in Table 2. Without auxiliary contrastive diffusion training, we observe a mean performance drop of 8.33% and 5.81% on MSE and CRPS over the whole benchmark. This notable decrease indicates that the dedicated denoising-based contrastive refinement can enhance the utilization efficiency of conditional temporal predictive information and yield a more genuine multivariate predictive distribution. Due to the restriction of computational costs, such contrastive gains on *Electricity* and *Traffic* datasets are relatively smaller. We can amplify contrastive benefits on large-scale datasets by increasing the batch size and negative number within an iteration in the future. Regarding the influence of composite channel-aware management in conditional denoiser, we replace the channel-wise DiT modules by the same depth of linear dense encoders and incur a full channel-independence architecture. The average reduction on MSE and CRPS over the whole test settings are 19.80% and 26.10%. This considerable drop reveals that the channel-mixing attention can empower the denoising network to integrate useful cross-variate temporal features in past observations and corrupted targets. Besides, the elevation degree induced by channel-centric DiT is consistent with the true variate correlations in real-world datasets. For instance, the per-



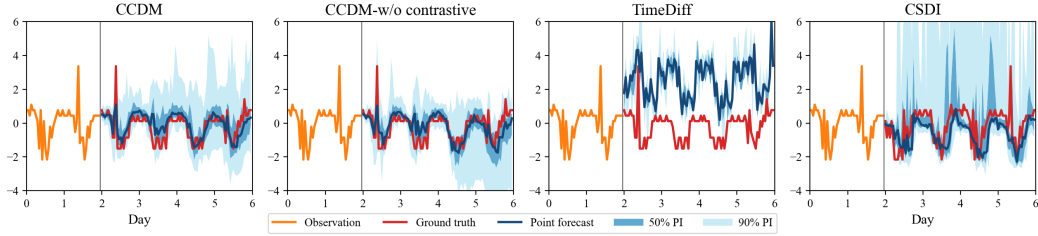


Figure 4: Comparison of generated point forecasts and prediction intervals on an Electricity channel.

formance decrease is less salient on `Electricity` dataset where the electricity consumption of different customers is not highly related to each other. Whilst on `ETTh1` and `Weather` datasets whose sensory measurements are heavily inter-correlated, the channel-mixing DiT can improve the diffusion forecasting capacity more vastly.

Table 2: Average MSE and CRPS degradation resulting from the ablation of denoising-based contrastive learning or channel-wise DiT module. Full results can be found in Appendix A.9.

Models	w/o contrastive refinement				w/o channel-wise DiT			
	MSE	Degradation	CRPS	Degradation	MSE	Degradation	CRPS	Degradation
ETTh1	0.5508	15.97%	0.3889	8.55%	0.5956	23.34%	0.5816	58.20%
Exchange	0.4966	11.52%	0.3403	5.24%	0.4924	12.18%	0.3555	11.00%
Weather	0.3816	13.00%	0.2695	4.77%	0.4843	40.28%	0.3336	28.92%
Appliance	1.0220	7.18%	0.5818	5.99%	1.1183	16.96%	0.7231	32.70%
Electricity	0.1887	1.20%	0.2144	1.57%	0.1973	5.71%	0.2137	1.25%
Traffic	0.8439	1.08%	0.4130	8.73%	1.0084	20.30%	0.4675	24.50%

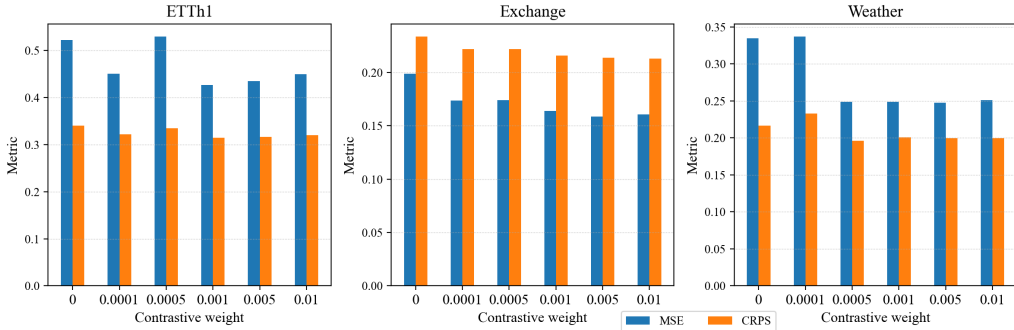


Figure 5: Forecasting results by varying contrastive weight  $\lambda$  on three datasets with  $H = 168$ .

#### 4.4 CONTRASTIVE REFINEMENT ANALYSIS

Below, we empirically investigate the efficacy of the devised denoising-based temporal contrastive refinement, including three vital factors for contrastive learning practice and its generality on other existing diffusion forecasters.

**Influence of contrastive weight  $\lambda$ .** The complementary step-wise denoising-based contrastive loss in 4 can enhance the alignment between diffusion generated forecasts and given temporal predictive information. To elucidate the impact of contrastive refinement in different degrees on original diffusion optimization, we escalate the contrastive weight  $\lambda$  in Eq. 5 from 0.0001 to 0.01 and display corresponding forecasting outcomes in Fig. 5. We can totally find that imposing contrastive regime on denoising diffusion training can indeed promote the generative forecasting capacity, and the gain margin moderately fluctuates among various weights and datasets. Roughly, a modest weight between 0.0005 and 0.005 can lead to better improvement. We also empirically observe that larger  $\lambda$  can accelerate the diffusion training convergence. See Appendix A.10 for more detailed analysis on the influence of negative number  $N$  and temperature  $\tau$ .

**Generality of contrastive training.** We add the step-wise denoising contrastive training presented in 4 to two existing diffusion forecasters to validate its generality on conditional time series diffusion

Table 3: Forecasting performance promotion induced by applying denoising-based contrastive training to two existing conditional diffusion forecasters.

Methods		TimeDiff				CSDI			
Metrics		MSE	Promotion	CRPS	Promotion	MSE	Promotion	CRPS	Promotion
ETTh	96	0.4143	-2.93%	0.3491	11.44%	0.6559	40.44%	0.4371	24.56%
	168	0.4715	-7.23%	0.3753	10.00%	0.5894	29.53%	0.3851	25.76%
	336	0.5073	-2.63%	0.4025	10.32%	0.9920	5.15%	0.5644	9.30%
	720	0.5291	6.19%	0.4338	14.44%	0.7744	23.18%	0.7010	-17.78%
Exchange	96	0.0901	18.54%	0.1722	26.69%	0.1589	37.71%	0.2082	28.23%
	168	0.1588	22.54%	0.2312	27.46%	0.4096	49.12%	0.3840	24.60%
	336	0.6345	-8.76%	0.4293	21.55%	0.5664	8.33%	0.4110	14.12%
	720	0.9735	-7.03%	0.6941	2.62%	1.3642	1.26%	0.6392	13.89%

learning. From the results shown in Table 3, it is obvious that CSDI’s generative forecasting ability can be further enhanced by contrastive diffusion training. Its hybrid attention network can represent complex temporal patterns more properly by handling more OOD negative samples. While for TimeDiff which owns extra pre-trained auto-regressive conditioning encoders, CRPS values constantly decrease but some unexpected increases appear on MSE. It may stem from the side effect of redundant contrastive procedure conveyed to the well-behaved deterministic pre-training strategy.

## 5 RELATED WORK

**Channel-oriented multivariate forecasting.** Recent progress on multivariate deterministic prediction (Liu et al., 2023; Lu et al., 2023; Chen et al., 2024a; Han et al., 2024) indicate that learning channel-centric temporal properties (including single-channel dynamics and cross-channel correlations) is of significant importance. Both channel-independent and channel-fusing time series processing are crucial to improve the forecasting performance. But the effectiveness of such channel manipulation structures is rarely investigated in diffusion-based multivariate probabilistic forecasting, where the extra influence of imposed channel noise in varying degrees should also be addressed. To tackle this barrier, we blend both channel-independent and channel-mixing modules in the conditional diffusion denoiser to boost its forecasting ability on multivariate cases.

**Time series diffusion models.** Diffusion models have been actively applied to tackle a wide scope of time series tasks, including synthesis (Yuan & Qiao, 2024; Narasimhan et al., 2024), forecasting (Rasul et al., 2021), imputation (Tashiro et al., 2021) and anomaly detection (Chen et al., 2023). Their common goal is to derive a high-quality conditional temporal distribution aligned with diverse input contexts, such as statistical properties in constrained generation (Coletta et al., 2024) and historical records. A valid solution is to inject useful temporal properties into iterative diffusion learning (Yuan & Qiao, 2024; Biloš et al., 2023) or to develop gradient-based guidance schemes (Coletta et al., 2024). But there are still rooms to enhance them from the aspect of training methods and denoiser architectures. To bridge this gap for multivariate forecasting, we exclusively design a channel-aware denoiser and explicitly enhance the predictive mutual information between past observations and future forecasts by an adapted temporal contrastive diffusion learning. Even though several works have applied contrastive diffusion to cross-modal content creation (Wang et al., 2024b; Zhu et al., 2022), its efficacy on time series generative modeling have not yet been well explored. And reasonable interpretations on such contrastive diffusion merits are also scanty. See Appendix A.2 for more detailed related work, which also covers universal temporal contrastive learning.

## 6 CONCLUSION

In this work, we propose the channel-aware contrastive conditional diffusion model named CCDM for probabilistic forecasts on multivariate time series. CCDM can capture intrinsic prediction-related temporal information hidden in observed conditioning time series using an efficient channel-centric denoiser architecture and information-maximizing denoising-based contrastive refinement. Extensive experiments demonstrate the exceptional forecasting capability of CCDM over existing time series diffusion models. In future work, we plan to reduce the training costs imposed by additional temporal contrastive learning, and extend this contrastive diffusion method to general time series analysis and other cross-domain synthesis tasks.

## ETHICS STATEMENT

Our work is only aimed at faithful multivariate probabilistic forecasting for human good, so there is no involvement of human subjects or conflict of interests as far as the authors are aware of.

## REFERENCES

- Juan Lopez Alcaraz and Nils Strodthoff. Diffusion-based time series imputation and forecasting with structured state space models. *Transactions on Machine Learning Research*, 2022.
- Marin Biloš, Kashif Rasul, Anderson Schneider, Yuriy Nevmyvaka, and Stephan Günnemann. Modeling temporal data as continuous functions with stochastic process diffusion. In *International Conference on Machine Learning*, pp. 2452–2470. PMLR, 2023.
- Defu Cao, Wen Ye, and Yan Liu. Timedit: General-purpose diffusion transformers for time series foundation model. In *ICML 2024 Workshop on Foundation Models in the Wild*, 2024.
- Jialin Chen, Jan Eric Lenssen, Aosong Feng, Weihua Hu, Matthias Fey, Leandros Tassioulas, Jure Leskovec, and Rex Ying. From similarity to superiority: Channel clustering for time series forecasting. *arXiv preprint arXiv:2404.01340*, 2024a.
- Minshuo Chen, Song Mei, Jianqing Fan, and Mengdi Wang. An overview of diffusion models: Applications, guided generation, statistical rates and optimization. *arXiv preprint arXiv:2404.07771*, 2024b.
- Ting Chen, Simon Kornblith, Mohammad Norouzi, and Geoffrey Hinton. A simple framework for contrastive learning of visual representations. In *International conference on machine learning*, pp. 1597–1607. PMLR, 2020.
- Yuhang Chen, Chaoyun Zhang, Minghua Ma, Yudong Liu, Ruomeng Ding, Bowen Li, Shilin He, Saravan Rajmohan, Qingwei Lin, and Dongmei Zhang. Imdiffusion: Imputed diffusion models for multivariate time series anomaly detection. *Proceedings of the VLDB Endowment*, 17(3): 359–372, 2023.
- Andrea Coletta, Sriram Gopalakrishnan, Daniel Borrajo, and Svitlana Vyetrenko. On the constrained time-series generation problem. *Advances in Neural Information Processing Systems*, 36, 2024.
- Jonathan Crabbé, Nicolas Huynh, Jan Pawel Stanczuk, and Mihaela van der Schaar. Time series diffusion in the frequency domain. In *Forty-first International Conference on Machine Learning*, 2024.
- Abhimanyu Das, Weihao Kong, Andrew Leach, Shaan K Mathur, Rajat Sen, and Rose Yu. Long-term forecasting with tide: Time-series dense encoder. *Transactions on Machine Learning Research*, 2023a.
- Abhimanyu Das, Weihao Kong, Rajat Sen, and Yichen Zhou. A decoder-only foundation model for time-series forecasting. *arXiv preprint arXiv:2310.10688*, 2023b.
- Jinliang Deng, Xuan Song, Ivor W Tsang, and Hui Xiong. The bigger the better? rethinking the effective model scale in long-term time series forecasting. *arXiv preprint arXiv:2401.11929*, 2024.
- Jonathan Dumas, Antoine Wehenkel, Damien Lanaspèze, Bertrand Cornélusse, and Antonio Sutera. A deep generative model for probabilistic energy forecasting in power systems: normalizing flows. *Applied Energy*, 305:117871, 2022.
- Patrick Esser, Sumith Kulal, Andreas Blattmann, Rahim Entezari, Jonas Müller, Harry Saini, Yam Levi, Dominik Lorenz, Axel Sauer, Frederic Boesel, et al. Scaling rectified flow transformers for high-resolution image synthesis. *arXiv preprint arXiv:2403.03206*, 2024.
- Xinyao Fan, Yueying Wu, Chang Xu, Yuhao Huang, Weiqing Liu, and Jiang Bian. Mg-tds: Multi-granularity time series diffusion models with guided learning process. *arXiv preprint arXiv:2403.05751*, 2024.

- Shibo Feng, Chunyan Miao, Zhong Zhang, and Peilin Zhao. Latent diffusion transformer for probabilistic time series forecasting. In *Proceedings of the AAAI Conference on Artificial Intelligence*, volume 38, pp. 11979–11987, 2024.
- Jean-Yves Franceschi, Aymeric Dieuleveut, and Martin Jaggi. Unsupervised scalable representation learning for multivariate time series. *Advances in neural information processing systems*, 32, 2019.
- Yuan Gao, Haokun Chen, Xiang Wang, Zhicai Wang, Xue Wang, Jinyang Gao, and Bolin Ding. Diffsformer: A diffusion transformer on stock factor augmentation. *arXiv preprint arXiv:2402.06656*, 2024.
- Lu Han, Xu-Yang Chen, Han-Jia Ye, and De-Chuan Zhan. Softs: Efficient multivariate time series forecasting with series-core fusion. *arXiv preprint arXiv:2404.14197*, 2024.
- Jonathan Ho, Ajay Jain, and Pieter Abbeel. Denoising diffusion probabilistic models. *Advances in neural information processing systems*, 33:6840–6851, 2020.
- Xingshuai Huang, Di Wu, and Benoit Boulet. Metaprobformer for charging load probabilistic forecasting of electric vehicle charging stations. *IEEE Transactions on Intelligent Transportation Systems*, 2023.
- Romain Ilbert, Ambroise Odonnat, Vasilii Feofanov, Aladin Virmaux, Giuseppe Paolo, Themis Palpanas, and Ievgen Redko. Unlocking the potential of transformers in time series forecasting with sharpness-aware minimization and channel-wise attention. *arXiv preprint arXiv:2402.10198*, 2024.
- Chiyu Jiang, Andre Cornman, Cheolho Park, Benjamin Sapp, Yin Zhou, Dragomir Anguelov, et al. Motiondiffuser: Controllable multi-agent motion prediction using diffusion. In *Proceedings of the IEEE/CVF Conference on Computer Vision and Pattern Recognition*, pp. 9644–9653, 2023.
- Marcel Kollovieh, Abdul Fatir Ansari, Michael Bohlke-Schneider, Jasper Zschiegner, Hao Wang, and Yuyang Bernie Wang. Predict, refine, synthesize: Self-guiding diffusion models for probabilistic time series forecasting. *Advances in Neural Information Processing Systems*, 36, 2024.
- Seunghan Lee, Taeyoung Park, and Kibok Lee. Soft contrastive learning for time series. In *The Twelfth International Conference on Learning Representations*, 2023.
- Lizao Li, Robert Carver, Ignacio Lopez-Gomez, Fei Sha, and John Anderson. Generative emulation of weather forecast ensembles with diffusion models. *Science Advances*, 10(13):eadk4489, 2024.
- Yan Li, Xinjiang Lu, Yaqing Wang, and Dejing Dou. Generative time series forecasting with diffusion, denoise, and disentanglement. *Advances in Neural Information Processing Systems*, 35: 23009–23022, 2022.
- Yuxin Li, Wenchao Chen, Xinyue Hu, Bo Chen, Mingyuan Zhou, et al. Transformer-modulated diffusion models for probabilistic multivariate time series forecasting. In *The Twelfth International Conference on Learning Representations*, 2023.
- Paul Pu Liang, Yun Cheng, Xiang Fan, Chun Kai Ling, Suzanne Nie, Richard Chen, Zihao Deng, Nicholas Allen, Randy Auerbach, Faisal Mahmood, et al. Quantifying & modeling multimodal interactions: An information decomposition framework. *Advances in Neural Information Processing Systems*, 36, 2024a.
- Paul Pu Liang, Zihao Deng, Martin Q Ma, James Y Zou, Louis-Philippe Morency, and Ruslan Salakhutdinov. Factorized contrastive learning: Going beyond multi-view redundancy. *Advances in Neural Information Processing Systems*, 36, 2024b.
- Lequan Lin, Zhengkun Li, Ruikun Li, Xuliang Li, and Junbin Gao. Diffusion models for time-series applications: a survey. *Frontiers of Information Technology & Electronic Engineering*, pp. 1–23, 2023.

- Yong Liu, Haixu Wu, Jianmin Wang, and Mingsheng Long. Non-stationary transformers: Exploring the stationarity in time series forecasting. *Advances in Neural Information Processing Systems*, 35:9881–9893, 2022.
- Yong Liu, Tengge Hu, Haoran Zhang, Haixu Wu, Shiyu Wang, Lintao Ma, and Mingsheng Long. itransformer: Inverted transformers are effective for time series forecasting. In *The Twelfth International Conference on Learning Representations*, 2023.
- Jiecheng Lu, Xu Han, and Shihao Yang. Arm: Refining multivariate forecasting with adaptive temporal-contextual learning. In *The Twelfth International Conference on Learning Representations*, 2023.
- Sai Shankar Narasimhan, Shubhankar Agarwal, Oguzhan Akcin, Sujay Sanghavi, and Sandeep Chinchali. Time weaver: A conditional time series generation model. *arXiv preprint arXiv:2403.02682*, 2024.
- Yuqi Nie, Nam H Nguyen, Phanwadee Sinthong, and Jayant Kalagnanam. A time series is worth 64 words: Long-term forecasting with transformers. In *The Eleventh International Conference on Learning Representations*, 2022.
- Aaron van den Oord, Yazhe Li, and Oriol Vinyals. Representation learning with contrastive predictive coding. *arXiv preprint arXiv:1807.03748*, 2018.
- William Peebles and Saining Xie. Scalable diffusion models with transformers. In *Proceedings of the IEEE/CVF International Conference on Computer Vision*, pp. 4195–4205, 2023.
- Kashif Rasul, Abdul-Saboor Sheikh, Ingmar Schuster, Urs M Bergmann, and Roland Vollgraf. Multivariate probabilistic time series forecasting via conditioned normalizing flows. In *International Conference on Learning Representations*, 2020.
- Kashif Rasul, Calvin Seward, Ingmar Schuster, and Roland Vollgraf. Autoregressive denoising diffusion models for multivariate probabilistic time series forecasting. In *International Conference on Machine Learning*, pp. 8857–8868. PMLR, 2021.
- David Salinas, Michael Bohlke-Schneider, Laurent Callot, Roberto Medico, and Jan Gasthaus. High-dimensional multivariate forecasting with low-rank gaussian copula processes. *Advances in neural information processing systems*, 32, 2019.
- Lifeng Shen and James Kwok. Non-autoregressive conditional diffusion models for time series prediction. In *International Conference on Machine Learning*, pp. 31016–31029. PMLR, 2023.
- Lifeng Shen, Weiyu Chen, and James Kwok. Multi-resolution diffusion models for time series forecasting. In *The Twelfth International Conference on Learning Representations*, 2023.
- Jiaming Song and Stefano Ermon. Understanding the limitations of variational mutual information estimators. In *International Conference on Learning Representations*, 2019.
- Yang Song, Jascha Sohl-Dickstein, Diederik P Kingma, Abhishek Kumar, Stefano Ermon, and Ben Poole. Score-based generative modeling through stochastic differential equations. *arXiv preprint arXiv:2011.13456*, 2020.
- Yusuke Tashiro, Jiaming Song, Yang Song, and Stefano Ermon. Csd: Conditional score-based diffusion models for probabilistic time series imputation. *Advances in Neural Information Processing Systems*, 34:24804–24816, 2021.
- Patara Trirat, Yooju Shin, Junhyeok Kang, Youngeun Nam, Jihye Na, Minyoung Bae, Joeun Kim, Byunghyun Kim, and Jae-Gil Lee. Universal time-series representation learning: A survey. *arXiv preprint arXiv:2401.03717*, 2024.
- Yao-Hung Hubert Tsai, Yue Wu, Ruslan Salakhutdinov, and Louis-Philippe Morency. Self-supervised learning from a multi-view perspective. In *International Conference on Learning Representations*, 2020.

- Feng Wang and Huaping Liu. Understanding the behaviour of contrastive loss. In *Proceedings of the IEEE/CVF conference on computer vision and pattern recognition*, pp. 2495–2504, 2021.
- Yihe Wang, Yu Han, Haishuai Wang, and Xiang Zhang. Contrast everything: A hierarchical contrastive framework for medical time-series. *Advances in Neural Information Processing Systems*, 36, 2024a.
- Yingheng Wang, Yair Schiff, Aaron Gokaslan, Weishen Pan, Fei Wang, Christopher De Sa, and Volodymyr Kuleshov. Infodiffusion: Representation learning using information maximizing diffusion models. In *International Conference on Machine Learning*, pp. 36336–36354. PMLR, 2023.
- Yongkang Wang, Xuan Liu, Feng Huang, Zhankun Xiong, and Wen Zhang. A multi-modal contrastive diffusion model for therapeutic peptide generation. In *Proceedings of the AAAI Conference on Artificial Intelligence*, volume 38, pp. 3–11, 2024b.
- Zhiyuan Wang, Xovee Xu, Weifeng Zhang, Goce Trajcevski, Ting Zhong, and Fan Zhou. Learning latent seasonal-trend representations for time series forecasting. *Advances in Neural Information Processing Systems*, 35:38775–38787, 2022.
- Gerald Woo, Chenghao Liu, Doyen Sahoo, Akshat Kumar, and Steven Hoi. Cost: Contrastive learning of disentangled seasonal-trend representations for time series forecasting. In *International Conference on Learning Representations*, 2021.
- Haixu Wu, Jiehui Xu, Jianmin Wang, and Mingsheng Long. Autoformer: Decomposition transformers with auto-correlation for long-term series forecasting. *Advances in neural information processing systems*, 34:22419–22430, 2021.
- Yunshu Wu, Yingtao Luo, Xianghao Kong, Evangelos E Papalexakis, and Greg Ver Steeg. Your diffusion model is secretly a noise classifier and benefits from contrastive training. *arXiv preprint arXiv:2407.08946*, 2024.
- Yiyuan Yang, Ming Jin, Haomin Wen, Chaoli Zhang, Yuxuan Liang, Lintao Ma, Yi Wang, Chenghao Liu, Bin Yang, Zenglin Xu, et al. A survey on diffusion models for time series and spatio-temporal data. *arXiv preprint arXiv:2404.18886*, 2024.
- Jinsung Yoon, Daniel Jarrett, and Mihaela Van der Schaar. Time-series generative adversarial networks. *Advances in neural information processing systems*, 32, 2019.
- Xinyu Yuan and Yan Qiao. Diffusion-ts: Interpretable diffusion for general time series generation. *arXiv preprint arXiv:2403.01742*, 2024.
- Ailing Zeng, Muxi Chen, Lei Zhang, and Qiang Xu. Are transformers effective for time series forecasting? In *Proceedings of the AAAI conference on artificial intelligence*, volume 37, pp. 11121–11128, 2023.
- Haoyi Zhou, Shanghang Zhang, Jieqi Peng, Shuai Zhang, Jianxin Li, Hui Xiong, and Wancai Zhang. Informer: Beyond efficient transformer for long sequence time-series forecasting. In *Proceedings of the AAAI conference on artificial intelligence*, volume 35, pp. 11106–11115, 2021.
- Tian Zhou, Ziqing Ma, Qingsong Wen, Xue Wang, Liang Sun, and Rong Jin. Fedformer: Frequency enhanced decomposed transformer for long-term series forecasting. In *International conference on machine learning*, pp. 27268–27286. PMLR, 2022.
- Ye Zhu, Yu Wu, Kyle Olszewski, Jian Ren, Sergey Tulyakov, and Yan Yan. Discrete contrastive diffusion for cross-modal music and image generation. In *The Eleventh International Conference on Learning Representations*, 2022.

## A APPENDIX

### A.1 PROOF FOR PROPOSITION 1

Below, we shed light on how to derive the upper bound of diffusion-induced probabilistic forecasting error shown in Proposition 1. We utilize the KL-divergence between the real distribution  $q^{te}(\mathbf{y}_0|\mathbf{x})$  of test time series and approximated predictive distribution  $p_\theta^{te}(\mathbf{y}_0|\mathbf{x})$  by conditional diffusion models to represent the probabilistic forecasting error

$$\mathcal{D}_{KL} [q^{te}(\mathbf{y}_0|\mathbf{x})||p_\theta^{te}(\mathbf{y}_0|\mathbf{x})] = \mathbb{E}_{q^{te}(\mathbf{y}_0|\mathbf{x})} [\log q^{te}(\mathbf{y}_0|\mathbf{x})] - \mathbb{E}_{q^{te}(\mathbf{y}_0|\mathbf{x})} [\log p_\theta^{te}(\mathbf{y}_0|\mathbf{x})]. \quad (8)$$

The first term in Eq. 8 is unrelated to conditional diffusion learning and thus can be prescribed as a constant  $C_1$  based on the information quantity of real test data

$$\mathbb{E}_{q^{te}(\mathbf{y}_0|\mathbf{x})} [\log q^{te}(\mathbf{y}_0|\mathbf{x})] = -\frac{1}{q^{te}(\mathbf{x})} \mathbb{E}_{q^{te}(\mathbf{y}_0|\mathbf{x})} [\log q^{te}(\mathbf{y}_0|\mathbf{x})] = -\frac{H(\mathbf{y}_0|\mathbf{x})}{q^{te}(\mathbf{x})} = C_1. \quad (9)$$

The second term Eq. 8 is the expected log-likelihood over  $q^{te}(\mathbf{y}_0|\mathbf{x})$ , which is identical to the learning objective of vanilla conditional diffusion models in (Ho et al., 2020). Akin to the step-wise denoising loss derivation in (Ho et al., 2020), we can obtain the upper bound of the error via Jensen's inequality and decompose it into  $K + 1$  items  $\mathcal{V}_0, \dots, \mathcal{V}_K$ :

$$\begin{aligned} -\mathbb{E}_{q^{te}(\mathbf{y}_0|\mathbf{x})} [\log p_\theta^{te}(\mathbf{y}_0|\mathbf{x})] &= -\mathbb{E}_{q^{te}(\mathbf{y}_0|\mathbf{x})} \left[ \log \int q^{te}(\mathbf{y}_{1:K}|\mathbf{y}_0) \frac{p_\theta^{te}(\mathbf{y}_{0:K}|\mathbf{x})}{q^{te}(\mathbf{y}_{1:K}|\mathbf{y}_0)} d\mathbf{y}_{1:K} \right] \\ &\leq -\mathbb{E}_{q^{te}(\mathbf{y}_0|\mathbf{x})} \left[ \mathbb{E}_{q^{te}(\mathbf{y}_{1:K}|\mathbf{y}_0)} \left[ \log \frac{p_\theta^{te}(\mathbf{y}_{0:K}|\mathbf{x})}{q^{te}(\mathbf{y}_{1:K}|\mathbf{y}_0)} \right] \right] \\ &= \mathbb{E}_{q^{te}(\mathbf{y}_0|\mathbf{x})} \left[ \mathcal{V}_0 + \sum_{k=2}^K \mathcal{V}_{k-1} + \mathcal{V}_K \right], \end{aligned} \quad (10)$$

where

$$\mathcal{V}_K = \mathcal{D}_{KL} [q^{te}(\mathbf{y}_K|\mathbf{y}_0)||p_\theta^{te}(\mathbf{y}_K|\mathbf{x})] = 0, \quad (11)$$

as  $q^{te}(\mathbf{y}_K|\mathbf{y}_0)$  and  $p_\theta^{te}(\mathbf{y}_K|\mathbf{x})$  are both standard Gaussian. And since the reverse transitions at each diffusion step can be shaped in explicit Gaussian forms, we can write out

$$\begin{aligned} \mathcal{V}_{k-1} &= \mathbb{E}_{q^{te}(\mathbf{y}_k|\mathbf{y}_0)} [\mathcal{D}_{KL} [q^{te}(\mathbf{y}_{k-1}|\mathbf{y}_k, \mathbf{y}_0)||p_\theta^{te}(\mathbf{y}_{k-1}|\mathbf{y}_k, \mathbf{x})]] \\ &= \mathbb{E}_{q^{te}(\mathbf{y}_k|\mathbf{y}_0)} \left[ \mathcal{D}_{KL} [\mathcal{N}(\mathbf{y}_{k-1}; \boldsymbol{\mu}_k(\mathbf{y}_k, \mathbf{y}_0), \tilde{\beta}_k \mathbf{I})||\mathcal{N}(\mathbf{y}_{k-1}; \boldsymbol{\mu}_\theta(\mathbf{y}_k, \mathbf{x}, k), \tilde{\beta}_k \mathbf{I})] \right] \\ &= \mathbb{E}_{q^{te}(\mathbf{y}_k|\mathbf{y}_0)} \left[ \frac{1}{2\tilde{\beta}_k^2} \left[ \|\boldsymbol{\mu}_\theta(\mathbf{y}_k, \mathbf{x}, k) - \boldsymbol{\mu}_k(\mathbf{y}_k, \mathbf{y}_0)\|_2^2 \right] \right] \\ &= \mathbb{E}_{\mathbf{y}_0, \boldsymbol{\epsilon}_k} \left[ \frac{1}{2\tilde{\beta}_k^2} \left[ \left\| \frac{1}{\sqrt{\alpha_k}} \left( \mathbf{y}_k - \frac{\beta_k}{\sqrt{1-\alpha_k}} \boldsymbol{\epsilon}_\theta(\mathbf{y}_k, \mathbf{x}, k) \right) - \frac{1}{\sqrt{\alpha_k}} \left( \mathbf{y}_k - \frac{\beta_k}{\sqrt{1-\alpha_k}} \boldsymbol{\epsilon}_k \right) \right\|_2^2 \right] \right] \\ &= \mathbb{E}_{\mathbf{y}_0, \boldsymbol{\epsilon}_k} \left[ \frac{\beta_k^2}{2\tilde{\beta}_k^2 \alpha_k (1-\alpha_k)} \left[ \|\boldsymbol{\epsilon}_\theta(\sqrt{\alpha_k} \mathbf{y}_0 + \sqrt{1-\alpha_k} \boldsymbol{\epsilon}_k, \mathbf{x}, k) - \boldsymbol{\epsilon}_k\|_2^2 \right] \right], \end{aligned} \quad (12)$$

where  $\tilde{\beta}_k = \frac{1-\alpha_{k-1}}{1-\alpha_k} \beta_k$  and  $\mathcal{V}_0$  is actually a special case of Eq. 12 when  $k = 1$

$$\begin{aligned} \mathcal{V}_0 &= -\mathbb{E}_{q(\mathbf{y}_1|\mathbf{y}_0)} [\log p_\theta(\mathbf{y}_0|\mathbf{y}_1, \mathbf{x})] \\ &= \mathbb{E}_{q(\mathbf{y}_1|\mathbf{y}_0)} \left[ \log(2\pi)^{\frac{HD}{2}} \tilde{\beta}_1 + \frac{1}{2\tilde{\beta}_1^2} \|\mathbf{y}_0 - \boldsymbol{\mu}_\theta(\mathbf{y}_1, \mathbf{x}, k=1)\|_2^2 \right] \\ &= \mathbb{E}_{\mathbf{y}_0, \boldsymbol{\epsilon}_1} \left[ \frac{\beta_1^2}{2\tilde{\beta}_1^2 \alpha_1 (1-\alpha_1)} \left[ \|\boldsymbol{\epsilon}_\theta(\sqrt{\alpha_1} \mathbf{y}_0 + \sqrt{1-\alpha_1} \boldsymbol{\epsilon}_1, \mathbf{x}, k=1) - \boldsymbol{\epsilon}_1\|_2^2 \right] \right] + C_2. \end{aligned} \quad (13)$$

Overall, if we let  $A_k = \frac{\beta_k^2}{2\beta_k^2\alpha_k(1-\bar{\alpha}_k)}$ ,  $C = C_1 + C_2$ , we can derive the ultimate upper bound of probabilistic forecasting error in a concise form as follows:

$$\mathcal{D}_{KL} [q^{te}(\mathbf{y}_0|\mathbf{x})||p_\theta^{te}(\mathbf{y}_0|\mathbf{x})] \leq \mathbb{E}_{\mathbf{x}, \mathbf{y}_0, \epsilon_k, k} \left[ A_k \left\| \epsilon_\theta \left( \sqrt{\bar{\alpha}_k} \mathbf{y}_0 + \sqrt{1 - \bar{\alpha}_k} \epsilon_k, \mathbf{x}, k \right) - \epsilon_k \right\|_2^2 \right] + C, \quad (14)$$

which finalizes the proof of Proposition 1. It shows that for unknown test time series, the diffusion-based generative forecasting performance is associated with the generalization capability of the trained conditional denoising network on total step-wise noise regression.

## A.2 ADDITIONAL DISCUSSIONS ON RELATED WORKS

**Channel-oriented multivariate forecasting.** How to properly manage various channel-centric temporal properties (i.e. single-channel dynamics and cross-channel correlations) has been attached greater importance in recent multivariate forecasting works (Chen et al., 2024a; Han et al., 2024) for two reasons. One is that traditional transformer-based models (Zhou et al., 2021; Wu et al., 2021; Zhou et al., 2022; Liu et al., 2022) only focus on improving the expressivity and efficiency of long-range temporal dependency, which can not obviously discriminate roles of disparate channels and entice some unsatisfactory outcomes. Besides, channel-independent predictors (Nie et al., 2022; Zeng et al., 2023; Das et al., 2023a) utilize a shared network to uniformly treat all channels and display that the single-channel separate prediction can outperform multi-channel mixing settings. Whilst this channel-independent structure fail to handle those complex temporal modes where the auxiliary information from other channels could also be helpful. Latest progress (Liu et al., 2023; Lu et al., 2023; Chen et al., 2024a; Han et al., 2024) reflect that both channel-independence and channel-fusion are crucial for versatile time series predictors. However, the significance of proper channel manipulation is rarely probed in multivariate diffusion forecasters, and the additional influence of channel noise imposed in different extents should also be considered. To tackle this barrier, we blend both channel-independence and channel-fusion modules in diffusion denoiser to boost its forecasting ability on multivariate cases.

**Time series diffusion models.** Due to the remarkable capacity to generate high-fidelity samples, diffusion models are actively exploited to grasp the stochastic dynamics and temporal correlations for a variety of time series tasks, including synthesis (Yuan & Qiao, 2024; Narasimhan et al., 2024), forecasting (Rasul et al., 2021), imputation (Tashiro et al., 2021) and anomaly detection (Chen et al., 2023). Common goals of these tasks are to derive a high-quality conditional temporal distribution aligned with diverse input contexts, such as statistical properties in constrained generation (Coletta et al., 2024) and historical records. To this end, the key challenge lies in how to design a potent temporal conditioning mechanism to empower the conditional backward generation. An intuitive way is to integrate useful temporal properties such as trend-seasonality (Yuan & Qiao, 2024), continuity (Biloš et al., 2023) and multi-scale modes (Shen et al., 2023; Fan et al., 2024) to empirically boost the utilization efficiency of conditioning data in the learnable denoising process. Another track is to develop gradient-based guidance schemes to satisfy given constraints via differentiable (Coletta et al., 2024) or objective-oriented optimization (Kollovich et al., 2024). Even this plethora of time series diffusion models, there are still rooms to enhance them from the aspect of training manners and denoiser architectures. To bridge this gap for multivariate forecasting, we exclusively design a channel-aware denoiser network and recast the problem of estimating conditional predictive distribution in the paradigm of mutual information maximization, which can enhance the consistency between past conditioning and future predicted time series. On top of original conditional likelihood maximization via step-wise noise regression, we adapt temporal contrastive learning to further augment conditional diffusion training. In future work, we hope to extend such innovations to benefit other time series analysis tasks.

**Temporal contrastive learning.** Time series contrastive learning primarily aims to obtain self-supervised universal temporal representations which can enable an array of downstream tasks with few shots (Trirat et al., 2024; Lee et al., 2023; Franceschi et al., 2019; Wang et al., 2024a). This line of research focus on developing efficient representation learning methods to pre-train temporal feature extractors in two vital senses, containing contrastive loss design and positive and negative sample pair construction. With respect to the deterministic time series prediction task, there also exist specialized decomposed contrastive pre-training approaches (Woo et al., 2021; Wang et al., 2022) to investigate disentangled seasonal and trend representations, which can relieve the subsequent pre-



diction on volatile temporal evolution. While in this work, we devise an end-to-end denoising-based contrastive learning to ameliorate conditional denoiser training rather than the common pre-training fashion on general temporal representation networks. We realize this contrastive refinement in an identical form of step-wise noise regression to vanilla diffusion. Moreover, we alter both temporal variations and point magnitudes in the time series augmentation stage, which can construct more useful negative samples for the contrastive denoiser improvement.

### A.3 NEGATIVE TIME SERIES AUGMENTATION

To enable contrastive learning, we employ two types of augmentation methods to produce negative multivariate time series  $\mathbf{y}_0^{(n)}$ . The first way is to alter the ground truth temporal variations of each univariate time series by patch shuffling, since recovering the correct temporal evolution is a vital challenge for time series diffusion models. As is shown in Fig. 6, we divide a given sequence into an array of sub-series patches and randomly shuffle their orders to change original temporal dynamics. The second way is to scale up or scale down the magnitudes of individual time points, as an ideal prediction interval should well cover every points without any of them falling outside. Thus, for each positive target  $\mathbf{y}_0$ , we uniformly sample a scaling factor  $a_d$  between  $[0, 0.5] \cup [1.5, 2.0]$  and impose it on each channel by  $a_d \cdot \mathbf{y}_0^d \in \mathbb{R}^H$ . We find both ways of generating negative samples would help the diffusion model learn more realistic time series samples.

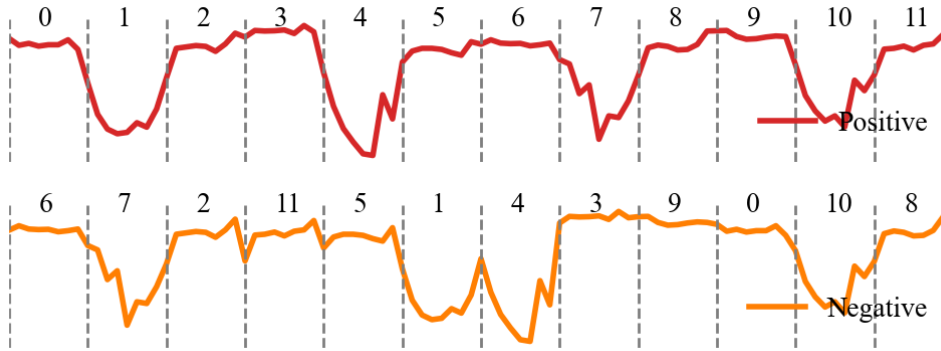


Figure 6: One diagram of the variation-based time series augmentation method.

### A.4 TRAINING ALGORITHM

We elucidate the step-wise denoising-based contrastive diffusion training algorithm in Algorithm 1.

---

#### Algorithm 1 Step-wise contrastive conditional diffusion training procedure.

---

**Input:** Lookback time series  $\mathbf{x} \in \mathbb{R}^{L \times D}$ ; target time series  $\mathbf{y}_0 \in \mathbb{R}^{H \times D}$ ; lookback length  $L$ ; prediction horizon  $H$ ; variate number  $D$ ; diffusion step number  $K$ ; negative sample number  $N$ ; contrastive loss weight  $\lambda$ ; temperature coefficient  $\tau$ ;

**repeat**

- 1: Draw step  $k \sim \mathbb{U}[1, \dots, K]$ .
- 2: Draw noise  $\epsilon \sim \mathcal{N}(\mathbf{0}, \mathbf{I})$  to calculate the naive diffusion loss  $\mathcal{L}_k^{denoise}$  in Eq. 1.
- 3: Draw noise  $\epsilon' \sim \mathcal{N}(\mathbf{0}, \mathbf{I})$  to calculate the denoising-based contrastive loss  $\mathcal{L}_k^{contrast}$  in Eq. 4.
- 4: Obtain a set of negative time series  $\{\mathbf{y}_0^n\}_{n=1}^N$  using the hybrid augmentation in Appendix A.3.
- 5: Compute the contrastive conditional diffusion loss  $\mathcal{L}_k^{CCDM} = \mathcal{L}_k^{denoise} + \lambda \mathcal{L}_k^{contrast}$  in Eq. 6.
- 6: Optimize the conditional denoising network  $\epsilon_\theta(\cdot)$  using the gradient  $\nabla_\theta \mathcal{L}_k^{CCDM}$ .

**until** converged

---

### A.5 DATASET DESCRIPTION

We present the dataset usage in Table 4, where the channel number  $D$ , sampling rate, train/val/test split size and own field are clarified. We also provide accessible repositories for these datasets below:

- 1) ETTh1: <https://github.com/zhouhaoyi/ETDataset>
- 2) Exchange: <https://github.com/laiguokun/multivariate-time-series-data>
- 3) Weather: <https://www.bgc-jena.mpg.de/wetter/>
- 4) Appliance: <https://archive.ics.uci.edu/dataset/374/appliances+energy+prediction>
- 5) Electricity: <https://archive.ics.uci.edu/dataset/321/electricityloadaddiagrams20112014>
- 6) Traffic: <https://pems.dot.ca.gov/>

Table 4: Detailed dataset description. Size indicates the split lengths of individual points for training, validation and testing division respectively.

Dataset	Variate number $D$	Sampling frequency	Split size	Field
ETTh1	7	Hourly	(8640, 2880, 2880)	Energy
Exchange	8	Daily	(5311, 758, 1517)	Finance
Weather	21	10min	(34560, 5760, 11520)	Weather
Appliance	28	10min	(13814, 1973, 3947)	Energy
Electricity	321	Hourly	(17280, 2880, 5760)	Energy
Traffic	862	Hourly	(11520, 2880, 2880)	Traffic

### A.6 EVALUATION METRICS

To assess the accuracy and reliability of estimated multivariate predictive distribution, we adopt two common metrics, i.e. MSE and CRPS to quantify both deterministic and probabilistic forecasting performance of generated prediction intervals. Assume  $\mathbf{y}_0$  is the ground-truth time series,  $\{\hat{\mathbf{y}}_0^{(s)}\}_{s=1}^S$  is the produced prediction set, and let its 50%-quantile trajectory  $\bar{\mathbf{y}}_0$  signify the point forecast, then two metrics can be calculated in a point-wise form over all channels and timestamps:

$$MSE = \frac{1}{HD} \|\mathbf{y}_0 - \bar{\mathbf{y}}_0\|_2^2; \quad (15)$$

$$CRPS = \frac{1}{HD} \sum_{d=1}^D \sum_{t=1}^H \int_R (F(\hat{y}_{td}) - \mathbb{I}\{y_{td} \leq \hat{y}_{td}\})^2 d\hat{y}_{td}; \quad (16)$$

where  $y_{td}$  indicates the  $t$ -th point value of the  $d$ -th univariate time series.  $F$  is the empirical cumulative distribution function.

### A.7 EXPERIMENTAL CONFIGURATIONS

In Table 5, we detail the conditional diffusion model configurations on different forecasting scenarios, including the channel-aware DiT compositions and diffusion noise scheduling. We simply preserve the layers of input and output channel-independent dense encoders identical to the depth of attention modules, i.e.  $n_{att} = n_{enc} = n_{dec} = 2$ . One observation is that the designed channel-centric conditional denoising network can be easily scalable with diverse forecasting scenarios by merely adjusting the hidden representation dimension  $e_{hid}$ , which changes compatibly with the prediction horizon  $H$ .

In Table 6, we shed light on the concrete contrastive training configurations for the main comparison outcomes presented in Table 1. We adopt the two-stage separate training on Weather, Electricity and Traffic datasets to reduce the training time and memory consumption. The best contrastive weight is chosen from  $\{0.001, 0.0005, 0.0001, 0.00005\}$ . Due to the GPU memory limitation, we have to turn down the negative sample number and batch size on Electricity and Traffic datasets with hundreds of channels, which could restrict the resulting final forecast performance. The initial learning rates are also displayed for the full reproduction on the newly adopted benchmark.

Table 5: Diffusion forecaster configurations on different forecasting setups.

Forecasting setup		DiT blocks			Noise schedule (quadratic)		
Lookback length $L$	Prediction horizon $H$	Depth $n_{att}$	Heads	Hidden dim $e_{hid}$	$\beta_1$	$\beta_K$	Steps $K$
48	96	2	8	128	0.0001	0.5	50
96	168	2	8	256	0.0001	0.2	100
192	336	2	8	512	0.0001	0.1	200
336	720	2	8	728	0.0001	0.1	200

Table 6: Contrastive training configurations corresponding to forecasting results in Table 1.

Setup	Contrastive weight $\lambda$	Negative number $N$	Batch size	Initial rate	Training mode	
ETTh1	96	0.001	64*2	32	0.001	End-to-end
	168	0.001	64*2	32	0.001	End-to-end
	336	0.001	64*2	32	0.0002	End-to-end
	720	0.001	64*2	32	0.0002	End-to-end
Exchange	96	0.001	64*2	32	0.001	End-to-end
	168	0.001	64*2	32	0.001	End-to-end
	336	0.001	64*2	32	0.0002	End-to-end
	720	0.001	64*2	32	0.0002	End-to-end
Weather	96	0.001	64*2	32	0.0001	Two-stage
	168	0.001	64*2	32	0.0001	Two-stage
	336	0.0001	64*2	32	0.00002	Two-stage
	720	0.001	64*2	32	0.00002	Two-stage
Appliance	96	0.001	64*2	32	0.001	End-to-end
	168	0.001	64*2	32	0.001	End-to-end
	336	0.0001	64*2	32	0.0002	End-to-end
	720	0.00005	64*2	32	0.0002	End-to-end
Electricity	96	0.0001	32*2	16	0.0001	Two-stage
	168	0.00005	32*2	12	0.0001	Two-stage
	336	0.00005	32*2	8	0.00002	Two-stage
	720	0.00005	20*2	8	0.00002	Two-stage
Traffic	96	0.0005	28*2	4	0.0001	Two-stage
	168	0.0001	22*2	4	0.0001	Two-stage
	336	0.00005	16*2	4	0.00002	Two-stage
	720	0.00005	12*2	4	0.00002	Two-stage

## A.8 COMPUTATIONAL TIME ANALYSIS

We compare the both training and inference time costs of disparate diffusion forecasters in Table 7. It is obvious that the auxiliary contrastive learning indeed aggravates the burden of vanilla denoising diffusion training for the sake of a higher quality of multivariate predictive distribution. Thus we adopt the two-stage separate strategy to accelerate the training process. The sequential generation procedure of our CCDM method is notably faster than other models, which indicates the designed channel-centric denoiser architecture can be efficiently scalable to diverse forecasting settings. Besides, the deterministic autoregressive pretraining in TimeDiff, hybrid attention layers in CSDI and point-wise amortized diffusion in TimeGrad can magnify their time consumption to different extents.

## A.9 FULL RESULTS ON ABLATION STUDY

We illuminate the full forecasting outcomes corresponding to the ablation study of Section 4.3 in Table 8. In a nutshell, the performance promotion margins derived from such denoiser architecture and contrastive refinement innovations vary among different forecasting scenarios. It still requires careful settings on channel-aware denoising networks and auxiliary contrastive training to achieve the optimal results for a specific time series field and prediction setup.

Table 7: Time cost comparison of diffusion forecasters on different sizes of prediction tasks. Both training time [s] of one epoch and inference time [ms] of one step are provided.

Size	CCDM		TimeDiff		CSDI		TimeGrad		
	Train [s]	Infer [ms]	Train [s]	Infer [ms]	Train [s]	Infer [ms]	Train [s]	Infer [ms]	
D=8	H=96	18.67	3.63	14.11	3.00	4.78	3.63	2.22	349.42
	H=168	28.11	4.37	18.56	3.00	6.33	3.58	3.89	603.05
	H=336	80.78	4.71	24.00	2.98	10.67	3.72	5.32	1163.55
	H=720	166.44	4.97	26.22	3.05	18.78	3.58	9.33	2571.37
D=28	H=96	66.67	3.76	25.44	4.00	34.89	3.76	7.67	374.23
	H=168	203.11	4.38	37.11	3.94	50.78	3.68	12.22	605.80
	H=336	441.74	4.71	33.22	4.29	97.22	3.66	21.67	1170.64
	H=720	903.00	4.75	34.67	4.50	181.56	6.45	50.22	2551.13
D=321	H=96	573.22	4.59	657.67	17.92	84.78	9.08	48.56	357.51
	H=168	1131.89	4.70	859.44	19.48	145.89	17.20	86.22	630.14
	H=336	3173.89	4.83	1190.33	20.61	376.11	47.77	171.44	1188.07
	H=720	4039.56	5.09	1269.56	22.71	546.67	70.13	330.67	2672.31
D=862	H=96	1466.14	4.54	185.78	46.67	104.22	25.12	80.56	369.04
	H=168	1884.77	4.52	193.89	47.89	118.33	47.71	146.67	620.23
	H=336	3202.85	5.17	284.89	49.09	228.44	96.06	289.11	1186.83
	H=720	4678.78	7.86	463.56	55.01	417.33	193.62	545.67	2591.93

## A.10 MORE ANALYSIS ON CONTRASTIVE REFINEMENT

**Influence of negative number  $N$ .** It is claimed in previous works on visual contrastive representation learning Oord et al. (2018); Chen et al. (2020) that a larger number of negative samples within a training iteration can bring out more informative latent features for downstream vision recognition tasks. To probe the influence of number of negative sample  $N$  on the specialized contrastive time series diffusion model for multivariate forecasting, we change  $N$  in the range from 16 to 256 and showcase pertaining outcomes in Fig. 7. We can observe that the optimal  $N$  is 192, 128 and 16 on three datasets and two quantitative metrics of each dataset exhibit distinctive changing trends. This phenomenon suggests that the real impact of negative sample number on contrastive training gains is relatively intractable, which is not amenable to the law in visual contrastive self-supervised pretraining. It could also be caused by the substantially smaller amount of training corpus in time series than images. We should determine the best number of negative instances in light of concrete data characteristics along with other training hyper-parameters.

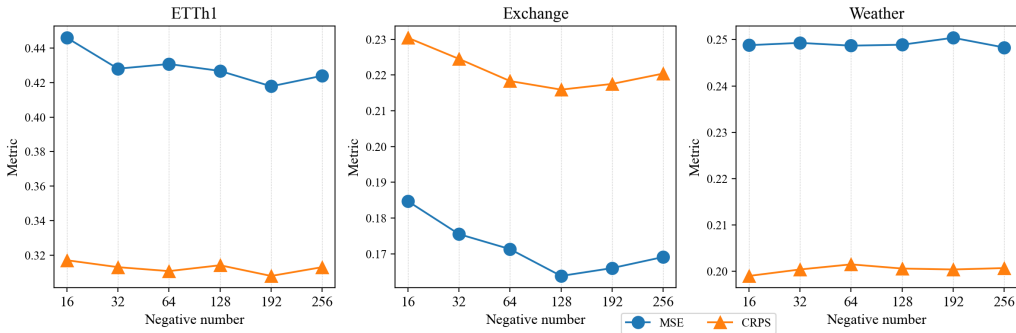


Figure 7: Forecasting results by different numbers of negative samples.

**Influence of temperature coefficient  $\tau$ .** The proposed denoising-based contrastive diffusion loss in Eq. 4 is in a canonical softmax form. According to the gradient analysis for the universal softmax-based contrastive loss in Wang & Liu (2021), the temperature  $\tau$  is a critical factor to control the penalty magnitude on various negative samples. To attain the contrastive improvement on conditional denoiser training, maintaining  $\tau$  within an appropriate interval is significant. We assign four values to  $\tau$  and illustrate quantitative results in Table 9. We can apparently observe that  $[0.05, 0.1]$  could be a reasonable range on ETTh1 and  $[0.1, 0.5]$  is also valid for other two datasets.

Table 8: Complete forecasting results by masking denoising-based temporal contrastive refinement or channel-mixing DiT blocks.

Methods		w/o contrastive refinement				w/o channel-wise DiT			
Metrics		MSE	Degradation	CRPS	Degradation	MSE	Degradation	CRPS	Degradation
ETTh1	96	0.4447	15.33%	0.3199	8.99%	0.3903	1.22%	0.2963	0.95%
	168	0.5223	22.40%	0.3402	8.27%	0.5800	35.93%	0.6674	112.41%
	336	0.6416	20.78%	0.3917	13.47%	0.5381	1.30%	0.4699	36.12%
	720	0.5944	5.35%	0.5038	3.45%	0.8740	54.91%	0.8928	83.33%
	Avg	0.5508	15.97%	0.3889	8.55%	0.5956	23.34%	0.5816	58.20%
Exchange	96	0.1057	16.80%	0.1677	8.54%	0.0959	5.97%	0.1598	3.43%
	168	0.1986	21.25%	0.2338	8.29%	0.2200	34.31%	0.2777	28.62%
	336	0.4532	2.84%	0.3557	1.14%	0.4735	7.44%	0.3870	10.04%
	720	1.2290	5.18%	0.6038	2.97%	1.1802	1.00%	0.5975	1.89%
	Avg	0.4966	11.52%	0.3403	5.24%	0.4924	12.18%	0.3555	11.00%
Weather	96	0.2825	5.84%	0.1936	1.68%	0.2919	9.37%	0.2012	5.67%
	168	0.3349	34.55%	0.2167	8.03%	0.4199	68.70%	0.2981	48.60%
	336	0.2932	2.16%	0.2313	2.44%	0.3825	33.28%	0.2873	27.24%
	720	0.6158	9.44%	0.4365	6.91%	0.8428	49.78%	0.5478	34.17%
	Avg	0.3816	13.00%	0.2695	4.77%	0.4843	40.28%	0.3336	28.92%
Appliance	96	0.7097	1.56%	0.4291	3.70%	0.7473	6.94%	0.4546	9.86%
	168	0.7313	16.71%	0.4374	8.81%	0.7853	25.33%	0.6070	51.00%
	336	0.9254	1.48%	0.5083	0.93%	1.0660	16.90%	0.6971	38.42%
	720	1.7215	8.97%	0.9525	10.50%	1.8744	18.65%	1.1336	31.51%
	Avg	1.0220	7.18%	0.5818	5.99%	1.1183	16.96%	0.7231	32.70%
Electricity	96	0.2142	1.90%	0.2266	3.85%	0.2296	9.23%	0.2198	0.73%
	168	0.1689	0.66%	0.2033	0.94%	0.1779	6.02%	0.2041	1.34%
	336	0.1714	1.84%	0.2035	1.04%	0.1744	3.62%	0.2048	1.69%
	720	0.2002	0.40%	0.2242	0.45%	0.2073	3.96%	0.2260	1.25%
	Avg	0.1887	1.20%	0.2144	1.57%	0.1973	5.71%	0.2137	1.25%
Traffic	96	1.0345	0.61%	0.4226	3.25%	1.2831	24.79%	0.4741	15.83%
	168	0.6936	0.80%	0.3113	1.17%	0.7682	11.64%	0.3869	25.74%
	336	0.6913	0.73%	0.3572	6.37%	0.8472	23.44%	0.4329	28.92%
	720	0.9561	2.18%	0.5610	24.14%	1.1351	21.31%	0.5762	27.51%
	Avg	0.8439	1.08%	0.4130	8.73%	1.0084	20.30%	0.4675	24.50%

Table 9: Forecasting results by different temperature coefficients.

Temperature $\tau$	ETTh1		Exchange		Weather	
	MSE	CRPS	MSE	CRPS	MSE	CRPS
0.05	0.4391	0.3124	0.1728	0.2216	0.2515	0.2015
0.1	0.4267	0.3142	0.1638	0.2159	0.2489	0.2006
0.5	0.4730	0.3252	0.1583	0.2152	0.2493	0.2022
1.0	0.5082	0.3389	0.2031	0.2449	0.2505	0.2025

## A.11 MORE SHOWCASES ON PREDICTION INTERVALS

In Fig. 8-13 below, we visualize more prediction intervals generated by the proposed CCDM on six datasets. The legend for each figure is identical to Fig. 4. For each task’s result visualization, we just display the first 7 or 8 variates and present two random samples on the  $L = 48$ ,  $H = 96$  setting.

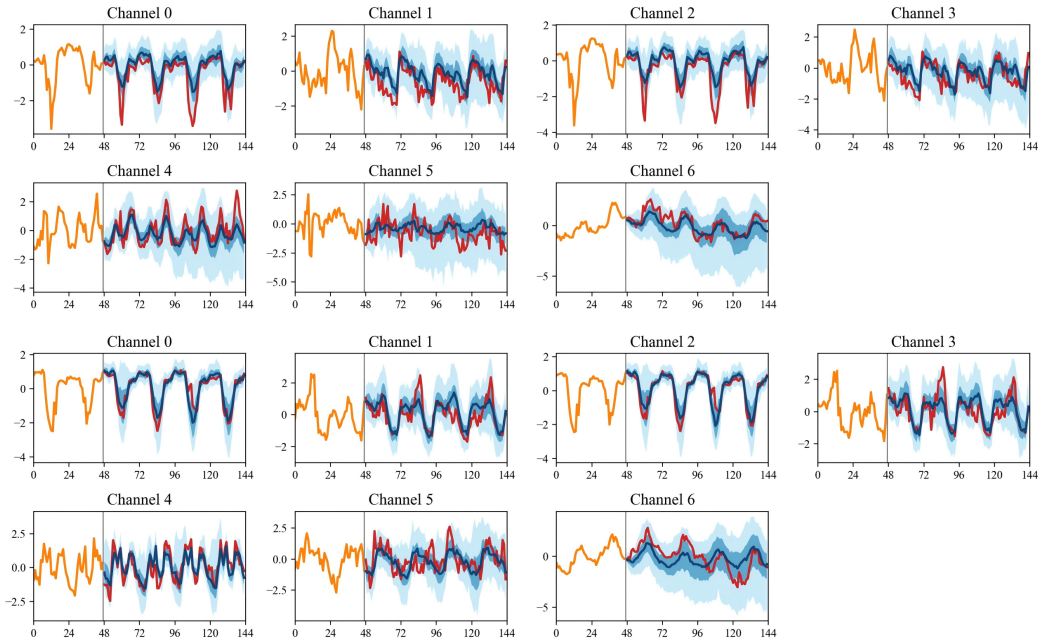


Figure 8: ETTh1 prediction intervals of total 7 channels.

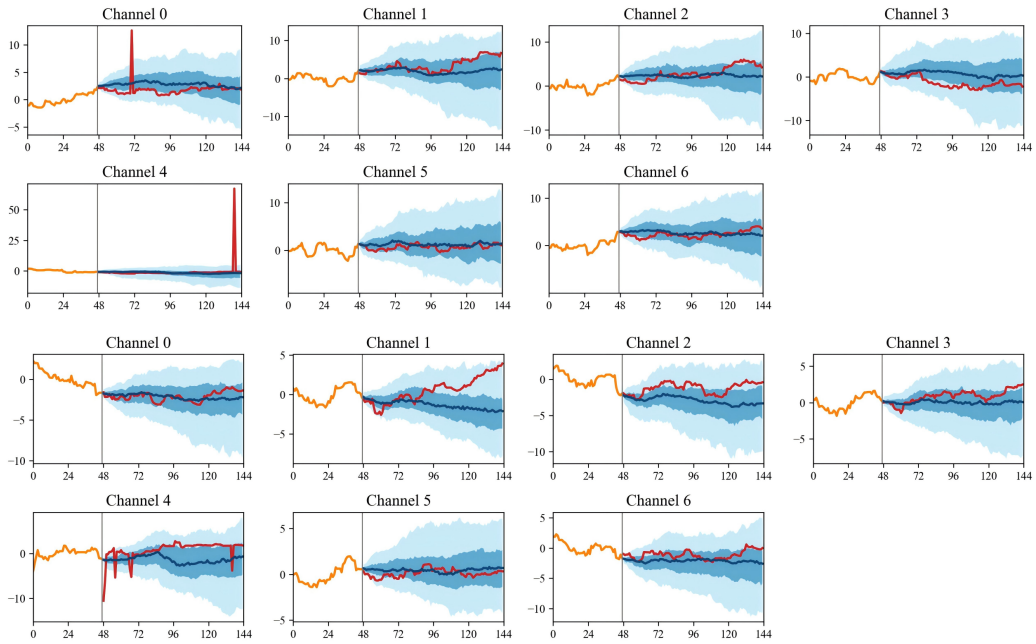


Figure 9: Exchange prediction intervals of total 7 channels.

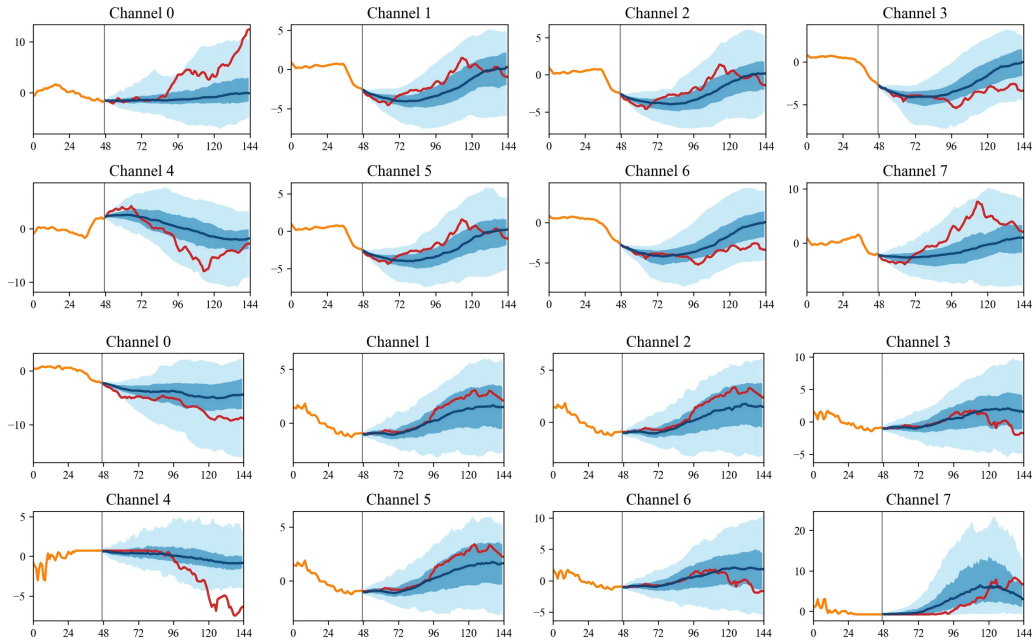


Figure 10: Weather prediction intervals of first 8 channels.

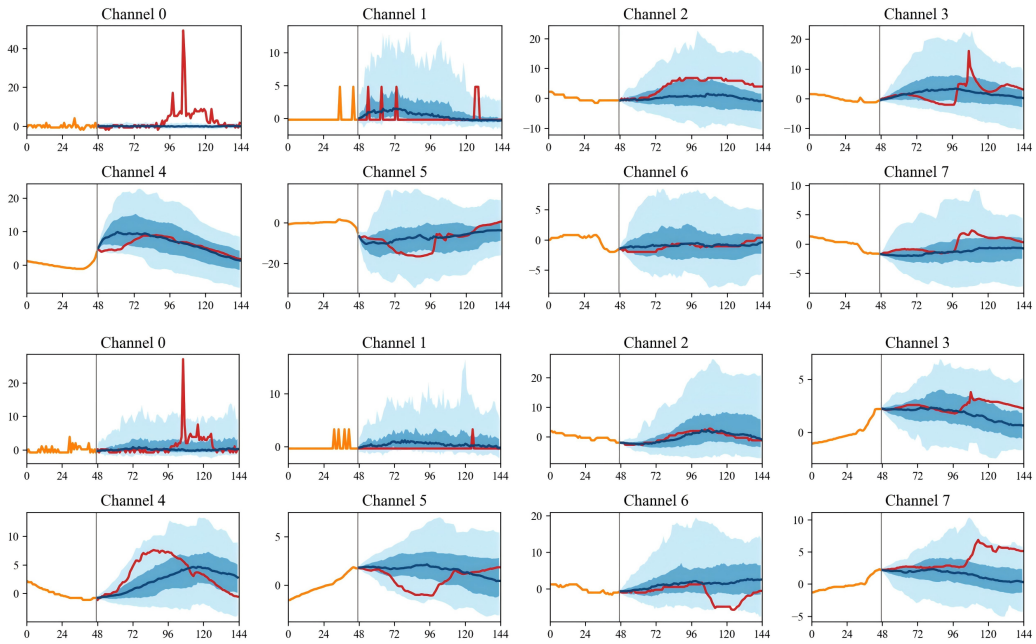


Figure 11: Appliance prediction intervals of first 8 channels.

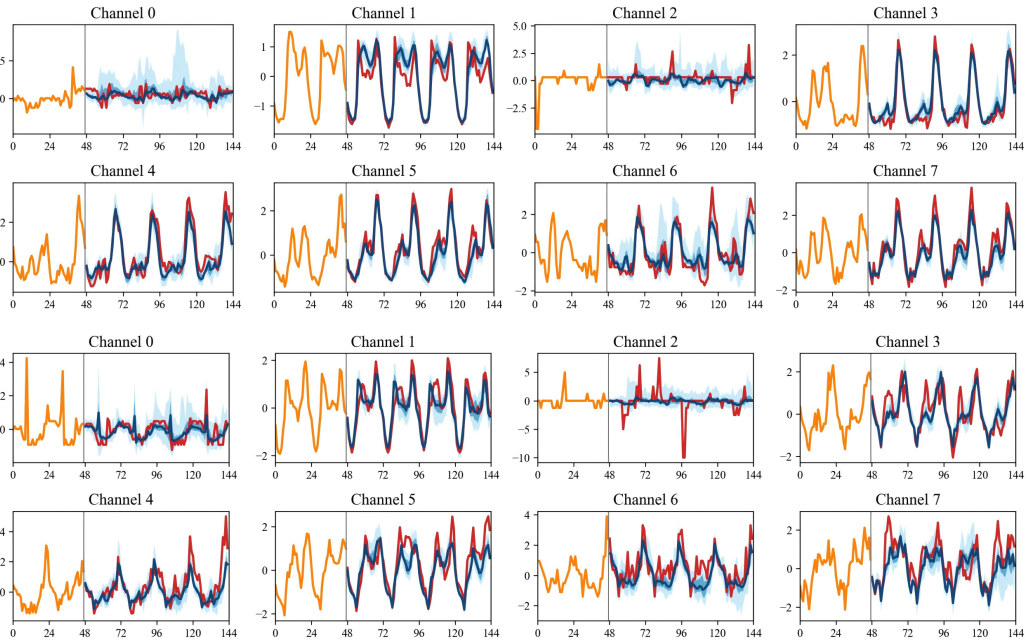


Figure 12: Electricity prediction intervals of first 8 channels.

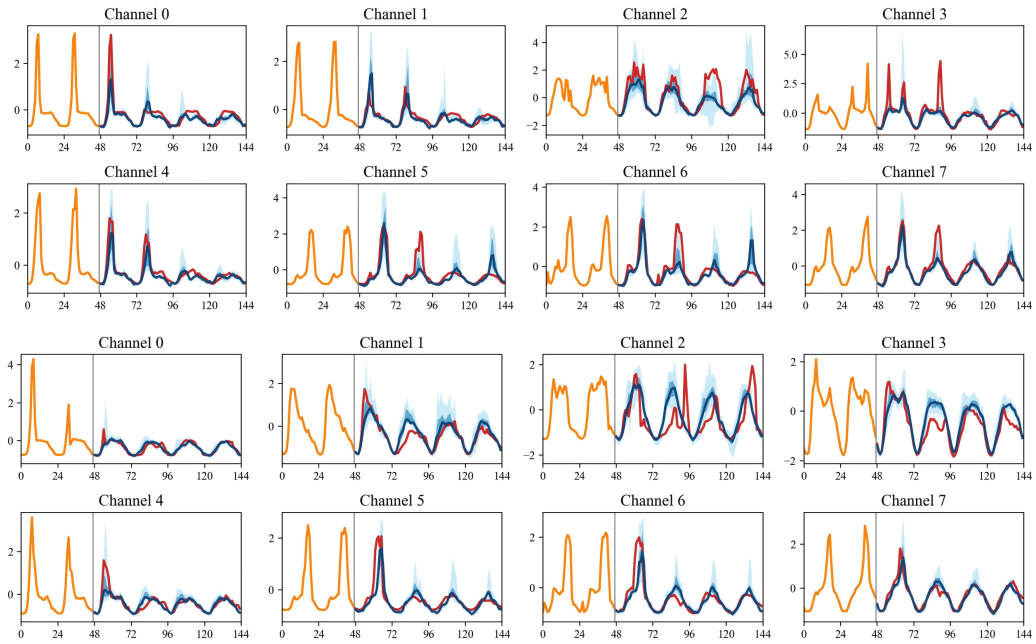


Figure 13: Traffic prediction intervals of first 8 channels.